



Synthesis, characterization and morphological studies of some novel siloxane-based block copolymeric materials containing organometallic as well as organic polyesteramides



Muhammad Saif Ullah Khan^a, Zareen Akhter^{a,*}, Naseer Iqbal^{b,c}, Mohammad Siddiq^a

^a Department of Chemistry, Quaid-i-Azam University, Islamabad 45320, Pakistan

^b Institute of Analytical and Food Chemistry, University of Vienna, Vienna, Austria

^c COMSATS Institute of Information Technology (CIIT), Lahore, Pakistan

ARTICLE INFO

Article history:

Received 15 May 2013

Received in revised form

24 July 2013

Accepted 4 August 2013

Keywords:

Organometallic polyesteramides

Block copolymers

Trifluoroacetylation

Molecular parameters

Moisture absorption

Surface morphology

ABSTRACT

A series of semi-aromatic diamine monomers (1,*m*-bis (4-amino benzoxy) alkanes; *m* = 2–6) having in-built ester linkages with variable methylene spacers were synthesized in two steps from aliphatic diols and *p*-nitrobenzoyl chloride and characterized by their melting points, elemental analysis, FTIR, ¹H and ¹³C NMR spectroscopic studies. The diamines were then polymerized *in-situ* with ferrocene-based organometallic and terephthaloyl- as well as isophthaloyl-based organic acyl chlorides along with telechelic polydimethylsiloxane oligomer to produce a novel set of ferrocene-containing siloxane-based block copolymers and their organic analogues. The corresponding polyesteramides of the synthesized copolymers, without siloxane segment, were also prepared for comparative studies. The structural features of the organometallic and organic block copolymers along with their respective polyesteramides were confirmed by their physical properties and spectroscopic studies. The molecular parameters of all these materials were determined by static laser light scattering (LLS) technique and glass transition temperatures (*T*_g) were obtained by differential scanning calorimetry (DSC). The materials were soluble in sulphuric acid and partially soluble in common organic solvents at room temperature, yet become readily soluble upon *N*-trifluoroacetylation. The morphological information of the synthesized materials was obtained by X-ray diffraction and surface studies (SEM and AFM).

© 2013 Elsevier B.V. All rights reserved.

1. Introduction

Polymer science has developed rapidly into an exciting area of high-tech materials research over the last few decades [1,2]. A major contribution to this transformation has been the infusion of creative ideas from synthetic organic chemists [1,2]. Block copolymers, which comprise two chemically dissimilar bonded polymer segments, are considered as an attractive category of polymeric materials because they combine the properties of both the parent polymers and offer the possibility of tailoring the physico-chemical and thermo-mechanical properties along with processability to obtain new engineering materials [3,4]. Siloxane-containing block copolymers, principally based on polydimethylsiloxane (PDMS), are particularly interesting because of the advantageous properties which include oxidative resistance, good biocompatibility, main chain flexibility and low surface

energy [3,4]. These polymeric systems are generally prepared by the incorporation of rigid structural segments such as polyamides, polyimides or polysulfones adjacent to the flexible siloxane units and can be utilized in many applications as specialized materials, such as gas separation membranes, biomaterials, photoresists, protective coatings, elastomers and emulsifiers [4,5]. Polycondensation is the most versatile technique for the synthesis of such copolymers. This is mainly due to the availability of a wide variety of well-defined reactive telechelic siloxane oligomers [3–5].

Polyesteramides are receiving much attention these days because these polymers may offer an interesting combination of properties: a high degradability caused by the ester linkages and good thermo-mechanical properties caused by the establishment of hydrogen bonds between amide groups [5–8]. These are of interest because of their excellent heat resistant and gas barrier properties [7] and have found a wide range of applications, such as disposable bags, agricultural films, drug carriers or matrix resins for biomedical materials [8,9].

Polyesteramides are generally prepared by solution, interfacial or melt polycondensation of diacids or their derivatives with amino

* Corresponding author. Tel.: +92 51 90642111; fax: +92 51 90642241.
E-mail address: zareenakhter@yahoo.com (Z. Akhter).

hydroxy compounds employing several condensing agents, such as thionyl chloride, diphenyl chlorophosphate, tosyl chloride and *N*-methyl imidazole [6–10]. However, the polycondensation reactions of diacid chlorides with aminophenols, diphenols or diamines containing preformed amide and ester groups have also been applied successfully for their synthesis [6–11]. Among different monomers utilized for the preparation of high-performance polymers, aromatic diamines are valuable building blocks which can induce desired modifications in the chemical nature of the macrochain [12–16]. Various rotatable segments such as ester group [12,13], ether moiety [14], sulfone linkage [15], methylene spacers [16], etc. can be introduced into the polymer backbones by structural modification of the diamine monomers. These flexible linkages increase the degree of freedom by reducing the segmental barrier and effectively disrupt the potential intermolecular interactions and thus enhance the solubility and processability of the resulting polymers [12–16].

The properties of the polymers can be modified by the incorporation of metals into their core structure [17]. The strategy can be useful in obtaining qualified polymeric materials with unusual and fascinating characteristics as there is great potential in combining the attributes of flexibility, versatility and solubility of the organic groups with the magnetic, electrical and optical properties of the metal [17,18]. Ferrocene entity, owing to its excellent thermal and photochemical stability as well as the unique and valuable redox behaviour, is an attractive scaffold for incorporating metal into polymeric structure [18]. Ferrocene-based polymers and copolymers are useful for a broad spectrum of applications, e.g. manufacture of electronic devices such as microelectrochemical diodes [19], formation of redox gels with charge transfer properties [20], for modification of electrodes [21], construction of amperometric biosensors [22], as precursors to ferromagnetic ceramics [23], in medical applications for cancer treatment [24] and also in the area of non-linear optical (NLO) materials [25].

Keeping in view the escalating performance characteristics demanded by block copolymers to meet the requirements of modern technological applications, the present study deals with a one-pot two-step synthesis of some novel polydimethylsiloxane-based hetero-atomic block copolymers containing ferrocene-based organometallic polyesteramides and their terephthaloyl- as well as isophthaloyl-based organic analogues using solution polycondensation technique. The corresponding polyesteramides of the synthesized block copolymers, without siloxane segment, were also prepared for comparison of properties. The diamine monomers used in the present work were of the general formulae; 1,*m*-bis(4-amino benzoyloxy)alkanes with variable aliphatic character ($m = 2-6$) and pre-formed ester linkages. The soft polydimethylsiloxane block used was of relatively higher molecular weight. It is believed that the properties of siloxane-based polymers can be tailored by merely changing the block length and/or the molecular weight of the siloxane oligomer [3,4,26]. The resulting organometallic materials as well as the organic analogues were characterized by various analytical techniques in order to elucidate their structures and explore their properties with respect to applications. These hard-soft polymers are expected to combine the advantageous properties of the parent polymers along with interesting new properties which enable them to be applicable in a number of technological fields such as layer by layer deposition of films for gas separation membranes, protective layers and also in biological applications [27–29].

2. Experimental

2.1. Materials and methods

All chemicals and reagents used were of highest purity unless otherwise mentioned. Ferrocene, aluminium chloride, acetyl

chloride, 4-nitrobenzoic acid, ethylene glycol, 1,3-propane diol, 1,4-butane diol, 1,5-pentane diol, 1,6-hexane diol, triethyl amine and 10% palladium on charcoal (Pd/C) were purchased from Fluka Chemie GmbH, Switzerland, and used without further purification. Anhydrous potassium carbonate, hydrazine monohydrate and thionyl chloride were obtained from Merck KGaA, Germany, and used as received. Bis (3-aminopropyl)-terminated polydimethylsiloxane (PDMS) $\text{H}_2\text{N}(\text{CH}_2)_3(\text{Me}_2\text{SiO})_y(\text{CH}_2)_3\text{NH}_2$ ($y = 360$), terephthaloyl chloride, isophthaloyl chloride and sodium hypochlorite solution (10%) were obtained from Sigma–Aldrich Chemie GmbH, Germany. Ethanol, *N,N'*-dimethyl formamide (DMF) and tetrahydrofuran (THF) were procured from Riedel-de Haën AG, Germany; toluene was obtained from Panreac Química S.L.U. Spain; and *m*-cresol and *n*-hexane were purchased from Fluka Chemie GmbH, Switzerland. Dichloromethane, diethyl ether, dimethyl sulfoxide (DMSO) and methanol were purchased from Merck KGaA, Germany. All solvents were freshly dried and distilled prior to use. Unless stated otherwise, all manipulations were conducted in an inert atmosphere created by vacuum line and dry N_2 gas. The progress of the reactions and purity of the products were monitored by thin layer chromatography on pre-coated Kieselgel 60HF TLC plates.

2.2. Measurements

The elemental (C, H, N) analysis of the synthesized compounds was performed using CHNS-932 LECO instrument. Melting temperatures of the products were determined on a Mel-Temp. (Mitamura Riken Kogyo.) apparatus using open capillary tubes and are uncorrected. The solid state Fourier transform infrared spectra were recorded on a Perkin Elmer Spectrum One (Ver. B) FTIR Spectrophotometer using KBr pellets. ^1H and ^{13}C NMR spectra were acquired with a Bruker 300 MHz ultrashield Spectrophotometer in appropriate solvent (DMSO- d_6 , CDCl_3 , THF- d_8). The effective field strength for ^{13}C NMR spectra was 75 MHz. Weight-average molar masses were determined on Brookhaven BI 200S instrument fitted with an argon-ion laser (Coherent Innova) with vertically polarized incident light of wavelength $\lambda = 637$ nm and a BI 9000 AT digital correlator. The refractive index increment (dn/dc) values were determined by using a high precision differential refractometer consisting of a laser light source, a position-sensitive detector, and a temperature-controlled refractometer cuvette and has wide linear detection range (± 0.035 RI units) with a resolution of 10^{-6} RI units, which is sufficient for determining the specific refractive index increment of most polymer solutions [30]. All the polymer solutions were clarified by a 0.45 μm millipore Teflon syringe filter prior to analysis. Water absorption studies were carried out following the ASTM D570-81 procedure [31]. The samples were placed in a vacuum oven at 80 °C until they attained a constant weight. These oven-dried pre-weighed samples (W_0) were then soaked in water for 72 h at room temperature (28 °C), dried by contacting with absorbent paper and weighed again (W_f). The percentage increase in weight of the sample was calculated by using the formula: $((W_f - W_0)/W_0) \times 100$. Wide-angle XRD analysis of the polymeric materials was carried out using a Philips 3040/60 X'Pert PRO diffractometer equipped with Cu- K_α radiation source. SEM and EDX analysis of the polymer surfaces were carried out using a JEOL JSM-6460 instrument coupled with Oxford EDS-7573. Samples were mounted with Al stubs using double-sided adhesive tapes and were coated with gold using a vacuum evaporator (JEOL-420) to make the surfaces conducting. AFM images of the polymeric materials were recorded on a Veeco Nanoscope IVa system in contact mode with Veeco SNL-10 silicon tips with a spring constant of 40 N m^{-1} and an onset pressure corresponding to a differential signal of 1 V on the photo diode. To obtain an image, 10 μL of the polymer materials were spin coated onto a sample disk and

scanned with scan rates in the range 1–2 Hz at room temperature (28 °C). DSC analysis of the synthesized polymeric materials was carried out using Mettler Toledo DSC 823e instrument at a rate of 10 °C min⁻¹ in nitrogen atmosphere.

2.3. Synthesis of ferrocene monomer

1,1'-Diacetyl ferrocene and 1,1'-ferrocene dicarboxylic acid were synthesized as reported by Rosenblum and Woodward [32] and Knobloch and Rauscher [33] respectively while 1,1'-ferrocene dicarbonyl chloride was prepared by an improved and efficient method described already by our group [34].

2.4. Synthesis of diamine monomers

The organic diamine monomers of the general formula 1,*m*-bis(4-amino benzoyloxy)alkanes (*m* = 2–6) were synthesized in two steps (Scheme 2) from *p*-nitrobenzoyl chloride, which was prepared according to the reported procedure [35]. The dinitro precursors were prepared in the first step and reduced to the diamine monomers in the second step as follows:

2.4.1. Synthesis of dinitro compounds (N-2, N-3, N-4, N-5 and N-6)

To a pre-baked three-neck round bottom glass flask equipped with a magnetic stirrer, reflux condenser and nitrogen inlet, a homogeneous solution of the corresponding diol (13.47 mmol) and triethyl amine (3.734 ml; 26.94 mmol) in anhydrous toluene (50 ml) was introduced. The reaction mixture was cooled to 10 °C and *p*-nitrobenzoyl chloride (5 g; 26.94 mmol) dissolved in toluene (15 ml) was added drop-wise over a period of 15 min. After complete addition, the mixture was refluxed for 3 h under inert conditions. The mixture was then allowed to cool and excess solvent was evaporated under vacuum. The solid obtained was isolated by filtration and stirred with distilled water for 1 h, again filtered and recrystallized with ethanol to afford the pure dinitro compound.

2.4.1.1. Preparation of 1,2-bis(4-nitrobenzoyloxy)ethane (N-2).

The dinitro species 1,2-bis(4-nitrobenzoyloxy)ethane (N-2) was prepared by the aforementioned general procedure using 1,2-ethane diol (0.75 ml; 13.47 mmol). Yield 85%, m.p. 136 °C. Elemental analysis for C₁₆H₁₂N₂O₈ (MW = 360) in wt% calc. C = 53.33, H = 3.33, N = 7.77 and found C = 52.95, H = 3.38, N = 7.92. FTIR (KBr pellet) in cm⁻¹: 3112, 3079 (w, C–H stretch Ar), 2958, 2856 (w, C–H stretch Al), 1720 (s, ester C=O stretch), 1608 (m, C=C stretch Ar), 1524, 1349 (s, NO₂ stretch), 837 (m, *p*-C₆H₄ bend). ¹H NMR (DMSO-*d*₆) in δ (ppm) and *J* (Hz): 8.42 (doub. 4H, *J* = 6.6, Ar–NO₂), 8.29 (doub. 4H, *J* = 6.8, Ar–CO), 4.77 (sing. 4H, CH₂O). ¹³C NMR (DMSO-*d*₆) in δ (ppm): 164.46 (2C, C=O), 150.75 (2C, Ar C1), 134.94 (2C, Ar C4), 130.84 (4C, Ar C3,3'), 123.66 (4C, Ar C2,2'), 63.36 (2C, OCH₂).

2.4.1.2. Preparation of 1,3-bis(4-nitrobenzoyloxy)propane (N-3).

1,3-Bis(4-nitrobenzoyloxy)propane (N-3) was prepared by the procedure described above using 1,3-propane diol (0.97 ml; 13.47 mmol). Yield 83%, m.p. 108 °C. Elemental analysis for C₁₇H₁₄N₂O₈ (MW = 374) in wt% calc. C = 54.54, H = 3.74, N = 7.48 and found C = 54.57, H = 3.63, N = 7.80. FTIR (KBr pellet) in cm⁻¹: 3116, 3094 (w, C–H stretch Ar), 2962, 2870 (w, C–H stretch Al), 1725 (s, ester C=O stretch), 1606 (m, C=C stretch Ar), 1527, 1356 (s, NO₂ stretch), 838 (m, *p*-C₆H₄ bend). ¹H NMR (DMSO-*d*₆) in δ (ppm) and *J* (Hz): 8.32 (doub. 4H, *J* = 7.2, Ar–NO₂), 8.14 (doub. 4H, *J* = 7.2, Ar–CO), 4.24 (trip. 4H, *J* = 6.9, CH₂O), 2.13 (pent. 2H, *J* = 7.3, CH₂). ¹³C NMR (DMSO-*d*₆) in δ (ppm): 166.26 (2C, C=O), 150.48 (2C, Ar C1), 136.83 (2C, Ar C4), 131.15 (4C, Ar C3,3'), 124.19 (4C, Ar C2,2'), 62.39 (2C, OCH₂), 27.41 (1C, CH₂).

2.4.1.3. Preparation of 1,4-bis(4-nitrobenzoyloxy)butane (N-4).

1,4-Bis(4-nitrobenzoyloxy)butane (N-4) was synthesized by the above mentioned procedure using 1,4-butane diol (1.19 ml; 13.47 mmol). Yield 84%, m.p. 168 °C. Elemental analysis for C₁₈H₁₆N₂O₈ (MW = 388) in wt% calc. C = 55.67, H = 4.12, N = 7.21 and found C = 55.85, H = 4.08, N = 7.59. FTIR (KBr pellet) in cm⁻¹: 3110, 3078 (w, C–H stretch Ar), 2944, 2854 (w, C–H stretch Al), 1718 (s, ester C=O stretch), 1606 (m, C=C stretch Ar), 1522, 1350 (s, NO₂ stretch), 842 (m, *p*-C₆H₄ bend). ¹H NMR (DMSO-*d*₆) in δ (ppm) and *J* (Hz): 8.32 (doub. 4H, *J* = 9.0, Ar–NO₂), 8.20 (doub. 4H, *J* = 9.0, Ar–CO), 4.41 (trip. 4H, *J* = 7.1, CH₂O), 1.91 (pent. 4H, *J* = 6.9, CH₂). ¹³C NMR (DMSO-*d*₆) in δ (ppm): 164.75 (2C, C=O), 150.70 (2C, Ar C1), 135.62 (2C, Ar C4), 131.08 (4C, Ar C3,3'), 124.34 (4C, Ar C2,2'), 65.65 (2C, OCH₂), 25.26 (2C, CH₂).

2.4.1.4. Preparation of 1,5-bis(4-nitrobenzoyloxy)pentane (N-5).

1,5-Bis(4-nitrobenzoyloxy)pentane (N-5) was prepared using 1,5-pentane diol (1.41 ml; 13.47 mmol) by the aforementioned general procedure. Yield 91%, m.p. 114 °C. Elemental analysis for C₁₉H₁₈N₂O₈ (MW = 402) in wt% calc. C = 56.72, H = 4.47, N = 6.96 and found C = 57.02, H = 4.48, N = 7.34. FTIR (KBr pellet) in cm⁻¹: 3112, 3082 (w, C–H stretch Ar), 2969, 2854 (w, C–H stretch Al), 1722 (s, ester C=O stretch), 1606 (m, C=C stretch Ar), 1524, 1351 (s, NO₂ stretch), 856 (m, *p*-C₆H₄ bend). ¹H NMR (DMSO-*d*₆) in δ (ppm) and *J* (Hz): 8.23 (doub. 4H, *J* = 8.4, Ar–NO₂), 8.13 (doub. 4H, *J* = 8.4, Ar–CO), 4.38 (trip. 4H, *J* = 6.9, CH₂O), 1.81 (pent. 4H, *J* = 7.3, OCH₂–CH₂–CH₂), 1.19 (pent. 2H, *J* = 7.4, CH₂–CH₂–CH₂). ¹³C NMR (DMSO-*d*₆) in δ (ppm): 167.29 (2C, C=O), 149.47 (2C, Ar C1), 141.34 (2C, Ar C4), 130.80 (4C, Ar C3,3'), 123.70 (4C, Ar C2,2'), 64.60 (2C, CH₂O), 28.74 (2C, OCH₂–CH₂–CH₂), 22.23 (1C, CH₂–CH₂–CH₂).

2.4.1.5. Preparation of 1,6-bis(4-nitrobenzoyloxy)hexane (N-6).

1,6-Bis(4-nitrobenzoyloxy)hexane (N-6) was synthesized by the general procedure using 1,6-hexane diol (1.58 g; 13.47 mmol). Yield 89%, m.p. 113 °C. Elemental analysis for C₂₀H₂₀N₂O₈ (MW = 416) in wt % calc. C = 57.69, H = 4.80, N = 6.73 and found C = 57.85, H = 4.71, N = 6.94. FTIR (KBr pellet) in cm⁻¹: 3117, 3081 (w, C–H stretch Ar), 2933, 2859 (w, C–H stretch Al), 1726 (s, ester C=O stretch), 1606 (m, C=C stretch Ar), 1526, 1349 (s, NO₂ stretch), 859 (m, *p*-C₆H₄ bend). ¹H NMR (DMSO-*d*₆) in δ (ppm) and *J* (Hz): 8.32 (doub. 4H, *J* = 8.7, Ar–NO₂), 8.16 (doub. 4H, *J* = 8.7, Ar–CO), 4.33 (trip. 4H, *J* = 5.9, CH₂O), 1.76 (pent. 4H, *J* = 7.1, OCH₂–CH₂–CH₂), 1.17 (pent. 4H, *J* = 7.1, CH₂–CH₂–CH₂). ¹³C NMR (DMSO-*d*₆) in δ (ppm): 166.29 (2C, C=O), 150.64 (2C, Ar C1), 137.09 (2C, Ar C4), 131.16 (4C, Ar C3,3'), 124.39 (4C, Ar C2,2'), 65.96 (2C, CH₂O), 28.58 (2C, CH₂–CH₂–CH₂O), 25.79 (2C, CH₂–CH₂–CH₂).

2.4.2. Synthesis of diamine monomers (D-2, D-3, D-4, D-5 and D-6)

A two-necked round bottom flask equipped with a magnetic stirrer and reflux condenser was charged with a suspension of the corresponding dinitro compound (12 mmol) and 10% Pd/C catalyst (0.1 g) in ethanol (40 ml) and brought to reflux. A solution hydrazine hydrate (15 ml) in ethanol (30 ml) was then added drop-wise over 30 min and the mixture was allowed to reflux for 10 h. The mixture was filtered to remove Pd–C and the filtrate was concentrated on a rotary vacuum evaporator to afford white solid precipitates which were washed thoroughly with distilled water and recrystallized from ethanol to obtain the pure diamine product.

2.4.2.1. Preparation of 1,2-bis(4-aminobenzoyloxy)ethane (D-2).

1,2-Bis(4-aminobenzoyloxy)ethane (D-2) was prepared by the aforementioned general procedure using 1,2-bis(4-nitrobenzoyloxy)ethane (N-2) (4.32 g; 12 mmol). Yield 73%, m.p. 205 °C. Elemental analysis for C₁₆H₁₆N₂O₄ (MW = 300) in wt% calc. C = 64.00, H = 5.33, N = 9.33 and found C = 64.30, H = 5.27, N = 9.62. FTIR (KBr pellet) in

cm^{-1} : 3431, 3351 (m, NH_2 stretch), 3231, 3044 (w, C–H stretch Ar), 2963, 2913 (w, C–H stretch Al), 1688 (s, ester C=O stretch), 1598 (m, C=C stretch Ar), 1515 (m, N–H bend), 841 (m, *p*- C_6H_4 bend). ^1H NMR (DMSO- d_6) in δ (ppm) and J (Hz): 7.63 (doub. 4H, $J = 8.7$, Ar–CO), 6.56 (doub. 4H, $J = 8.7$, Ar– NH_2), 5.96 (sing. 4H, NH_2), 4.682 (sing. 4H, CH_2O). ^{13}C NMR (DMSO- d_6) in δ (ppm): 166.53 (2C, C=O), 152.90 (2C, Ar C1), 130.78 (4C, Ar C3,3'), 118.31 (2C, Ar C4), 114.15 (4C, Ar C2,2'), 63.91 (2C, CH_2O).

2.4.2.2. Preparation of 1,3-bis(4-aminobenzoyloxy)propane (D-3).

1,3-Bis(4-aminobenzoyloxy)propane (D-3) was synthesized by the general procedure described above by reducing 1,3-bis(4-nitrobenzoyloxy)propane (N-3) (4.5 g; 12 mmol). Yield 76%, m.p. 125.2 °C. Elemental analysis for $\text{C}_{17}\text{H}_{18}\text{N}_2\text{O}_4$ (MW = 314) in wt% calc. C = 64.97, H = 5.73, N = 8.92 and found C = 64.40, H = 5.67, N = 9.10. FTIR (KBr pellet) in cm^{-1} : 3394, 3341 (m, NH_2 stretch), 3239, 2977 (w, C–H stretch Ar), 2946, 2869 (w, C–H stretch Al), 1693 (s, ester C=O stretch), 1600 (m, C=C stretch Ar), 1515 (m, N–H bend), 839 (m, *p*- C_6H_4 bend). ^1H NMR (DMSO- d_6) in δ (ppm) and J (Hz): 7.64 (doub. 4H, $J = 9.0$, Ar–CO), 6.53 (doub. 4H, $J = 9.0$, Ar– NH_2), 5.957 (sing. 4H, NH_2), 4.22 (trip. 4H, $J = 6.4$, OCH_2), 2.07 (pent. 2H, $J = 6.5$, CH_2). ^{13}C NMR (DMSO- d_6) in δ (ppm): 166.64 (2C, C=O), 153.11 (2C, Ar C1), 130.87 (4C, Ar C3,3'), 118.20 (2C, Ar C4), 113.75 (4C, Ar C2,2'), 64.66 (2C, OCH_2), 25.27 (1C, CH_2).

2.4.2.3. Preparation of 1,4-bis(4-aminobenzoyloxy)butane (D-4).

1,4-Bis(4-aminobenzoyloxy)butane (D-4) was prepared by reduction of 1,4-bis(4-nitrophenoxy)butane (N-4) (4.66 g; 12 mmol) using the above mentioned procedure. Yield 79%, m.p. 195.2 °C. Elemental analysis for $\text{C}_{18}\text{H}_{20}\text{N}_2\text{O}_4$ (MW = 328) in wt% calc. C = 65.85, H = 6.09, N = 8.53 and found C = 65.35, H = 6.17, N = 8.88. FTIR (KBr pellet) in cm^{-1} : 3463, 3367 (m, NH_2 stretch), 3245, 3030 (w, C–H stretch Ar), 2961, 2918 (w, C–H stretch Al), 1677 (s, ester C=O stretch), 1602 (m, C=C stretch Ar), 1519 (m, N–H bend), 835 (m, *p*- C_6H_4 bend). ^1H NMR (DMSO- d_6) in δ (ppm) and J (Hz): 7.63 (doub. 4H, $J = 8.7$, Ar–CO), 6.58 (doub. 4H, $J = 8.7$, Ar– NH_2), 5.96 (sing. 4H, NH_2), 4.20 (trip. 4H, $J = 6.6$, CH_2O), 1.78 (pent. 4H, $J = 6.5$, CH_2). ^{13}C NMR (DMSO- d_6) in δ (ppm): 166.37 (2C, C=O), 152.82 (2C, Ar C1), 130.94 (4C, Ar C3,3'), 117.31 (2C, Ar C4), 113.79 (4C, Ar C2,2'), 64.57 (2C, OCH_2), 25.36 (2C, CH_2).

2.4.2.4. Preparation of 1,5-bis(4-aminobenzoyloxy)pentane (D-5).

1,5-Bis(4-aminobenzoyloxy)pentane (D-5) was prepared by the above mentioned procedure using 1,5-bis(4-nitrobenzoyloxy)pentane (N-5) (4.82 g; 12 mmol). Yield 80%, m.p. 132 °C. Elemental analysis for $\text{C}_{19}\text{H}_{22}\text{N}_2\text{O}_4$ (MW = 342) in wt% calc. C = 64.00, H = 5.33, N = 9.33 and found C = 64.30, H = 5.27, N = 9.62. FTIR (KBr pellet) in cm^{-1} : 3432, 3336 (m, NH_2 stretch), 3214, 3070 (w, C–H stretch Ar), 2965, 2928 (w, C–H stretch Al), 1694 (s, ester C=O stretch), 1597 (m, C=C stretch Ar), 1515 (m, N–H bend), 843 (m, *p*- C_6H_4 bend). ^1H NMR (DMSO- d_6) in δ (ppm) and J (Hz): 7.62 (doub. 4H, $J = 8.7$, Ar–CO), 6.57 (doub. 4H, $J = 8.4$, Ar– NH_2), 5.94 (sing. 4H, NH_2), 4.17 (trip. 4H, $J = 7.1$, CH_2O), 1.71 (pent. 4H, $J = 7.0$, $\text{OCH}_2\text{—CH}_2\text{—CH}_2$), 1.48 (pent. 2H, $J = 7.1$, $\text{CH}_2\text{—CH}_2\text{—CH}_2$). ^{13}C NMR (DMSO- d_6) in δ (ppm): 166.36 (2C, C=O), 153.89 (2C, Ar C1), 131.49 (4C, Ar C3,3'), 116.84 (2C, Ar C4), 113.12 (4C, Ar C2,2'), 63.81 (2C, OCH_2), 28.52 (2C, $\text{OCH}_2\text{—CH}_2\text{—CH}_2$), 22.69 (1C, $\text{CH}_2\text{—CH}_2\text{—CH}_2$).

2.4.2.5. Preparation of 1,6-bis(4-aminobenzoyloxy)hexane (D-6).

1,6-Bis(4-aminobenzoyloxy)hexane (D-6) was prepared by the general procedure using 1,6-bis(4-nitrobenzoyloxy)hexane (N-6) (5 g; 12 mmol). Yield 78%, m.p. 166 °C. Elemental analysis for $\text{C}_{20}\text{H}_{24}\text{N}_2\text{O}_4$ (MW = 356) in wt% calc. C = 67.42, H = 6.74, N = 7.86 and found C = 66.83, H = 6.49, N = 8.03. FTIR (KBr pellet) in cm^{-1} : 3426, 3338 (m, NH_2 stretch), 3219, 3070 (w, C–H stretch Ar), 2942,

2860 (w, C–H stretch Al), 1685 (s, ester C=O stretch), 1597 (m, C=C stretch Ar), 1514 (m, N–H bend), 843 (m, *p*- C_6H_4 bend). ^1H NMR (DMSO- d_6) in δ (ppm) and J (Hz): 7.63 (doub. 4H, $J = 8.7$, Ar–CO), 6.55 (doub. 4H, $J = 8.7$, Ar– NH_2), 5.95 (sing. 4H, NH_2), 4.14 (trip. 4H, $J = 6.7$, CH_2O), 1.67 (pent. 4H, $J = 6.9$, $\text{CH}_2\text{—CH}_2\text{—CH}_2\text{O}$), 1.424 (pent. 4H, $J = 6.9$, $\text{CH}_2\text{—CH}_2\text{—CH}_2$). ^{13}C NMR (DMSO- d_6) in δ (ppm): 167.27 (2C, C=O), 153.52 (2C, Ar C1), 131.57 (4C, Ar C3,3'), 116.74 (2C, Ar C4), 113.49 (4C, Ar C2,2'), 64.36 (2C, CH_2O), 28.36 (2C, $\text{CH}_2\text{—CH}_2\text{—CH}_2\text{O}$), 25.44 (2C, $\text{CH}_2\text{—CH}_2\text{—CH}_2$).

2.5. Synthesis of block copolymers

In a two-necked pre-baked round-bottom flask, the corresponding diamine (1.84 mmol) was dissolved freshly dried hot THF (15 ml) and treated with triethylamine (10 ml) under an inert atmosphere. The temperature was lowered to 0 °C using an ice bath and 1,1'-ferrocenedicarbonyl chloride (0.600 g, 1.92 mmol) in dry THF (10 ml) was added drop-wise with vigorous stirring over a period of 30 min. The temperature was slowly raised to room temperature and PDMS (2 g; 0.076 mmol) dissolved in dry THF (10 ml) was added drop-wise to the mixture. The mixture was then allowed to reflux for 72 h. After completion of the reaction, the reaction mixture was cooled to ambient temperature and poured into an excess of methanol. The precipitated product was then collected by filtration and washed several times with methanol and hot *n*-hexane. The resulting product was dried in vacuum for 24 h. The organic analogues were synthesized by similar procedure using terephthaloyl chloride and isophthaloyl chloride. Synthesis of these copolymers is summarized in Scheme 3.

2.5.1. FcBC-2

Brown sticky solid; yield 68%. FT-IR (KBr pellet) in ν (cm^{-1}): 3293 (m, N–H stretch), 3089, 3027 (w, C–H stretch Ar), 2936, 2851 (w, C–H stretch Al), 1711 (s, ester C=O stretch), 1653 (s, amide-I), 1531 (s, amide-II), 1261 (s, Si– CH_3), 1099, 1014 (s, Si–O–Si stretch), 839 (m, C_6H_4 bend), 497 (m, Fe–Cp). ^1H NMR in δ (ppm): 0.11 (sing. SiCH_3), 5.09–4.54 (br. 8H, Cp), 7.48–6.54 (mult. 8H, Ar), 4.24 (sing. 4H, OCH_2).

2.5.2. FcBC-3

Brown sticky solid; yield 66%. FT-IR (KBr pellet) in ν (cm^{-1}): 3301 (m, N–H stretch), 3171, 3053 (w, C–H stretch Ar), 2937, 2823 (w, C–H stretch Al), 1713 (s, ester C=O stretch), 1654 (s, amide-I), 1537 (s, amide-II), 1262 (s, Si– CH_3), 1097, 1019 (s, Si–O–Si stretch), 831 (m, C_6H_4 bend), 500 (m, Fe–Cp). ^1H NMR in δ (ppm) and J (Hz): 0.14 (sing. SiCH_3), 5.03–4.51 (br. 8H, Cp), 7.60–6.49 (mult. 8H, Ar), 4.21 (trip. 4H, $J = 7.4$, OCH_2), 1.98 (pent. 2H, $J = 7.5$, CH_2).

2.5.3. FcBC-4

Brown sticky solid; yield 65%. FT-IR (KBr pellet) in ν (cm^{-1}): 3314 (m, N–H stretch), 3133, 3051 (w, C–H stretch Ar), 2949, 2866 (w, C–H stretch Al), 1709 (s, ester C=O stretch), 1653 (s, amide-I), 1539 (s, amide-II), 1260 (s, Si– CH_3), 1100, 1018 (s, Si–O–Si stretch), 829 (m, C_6H_4 bend), 495 (m, Fe–Cp). ^1H NMR in δ (ppm) and J (Hz): 0.17 (sing. SiCH_3), 5.11–4.47 (br. 8H, Cp), 7.46–6.41 (mult. 8H, Ar), 4.13 (trip. 4H, $J = 7.3$, OCH_2), 1.87 (pent. 4H, $J = 7.3$, CH_2).

2.5.4. FcBC-5

Dark brown sticky solid; yield 67%. FT-IR (KBr pellet) in ν (cm^{-1}): 3317 (m, N–H stretch), 3146, 3073 (w, C–H stretch Ar), 2957, 2861 (w, C–H stretch Al), 1711 (s, ester C=O stretch), 1651 (s, amide-I), 1531 (s, amide-II), 1262 (s, Si– CH_3), 1099, 1017 (s, Si–O–Si stretch), 836 (m, C_6H_4 bend), 497 (m, Fe–Cp). ^1H NMR in δ (ppm) and J (Hz): 0.13 (sing. SiCH_3), 5.04–4.49 (br. 8H, Cp), 7.45–6.43

(mult. 8H, Ar), 4.21 (trip. 4H, $J = 7.2$, OCH₂), 1.74–1.48 (mult. 6H, CH₂).

2.5.5. FcBC-6

Dark brown sticky solid; yield 68%. FT-IR (KBr pellet) in ν (cm⁻¹): 3299 (m, N–H stretch), 3139, 3049 (w, C–H stretch Ar), 2933, 2847 (w, C–H stretch Al), 1707 (s, ester C=O stretch), 1652 (s, amide-I), 1528 (s, amide-II), 1262 (s, Si–CH₃), 1100, 1021 (s, Si–O–Si stretch), 829 (m, C₆H₄ bend), 503 (m, Fe–Cp). ¹H NMR in δ (ppm) and J (Hz): 0.15 (sing. SiCH₃), 4.97–4.53 (br. 8H, Cp), 7.43–6.27 (mult. 8H, Ar), 4.17 (trip. 4H, $J = 7.3$, OCH₂), 1.64–1.49 (mult. 8H, CH₂). LLS: $M_w = 8.76 \times 10^6$ g mol⁻¹; $\langle R_g \rangle = 31$ nm; $A_2 = 5.90 \times 10^{-5}$ cm³ mol g⁻².

2.5.6. TBC-2

White sticky solid; yield 61%. FT-IR (KBr pellet) in ν (cm⁻¹): 3313 (m, N–H stretch), 3112, 3073 (w, C–H stretch Ar), 2937, 2880 (w, C–H stretch Al), 1706 (s, ester C=O stretch), 1647 (s, amide-I), 1529 (s, amide-II), 1261 (s, Si–CH₃), 1097, 1017 (s, Si–O–Si stretch), 831 (m, C₆H₄ bend). ¹H NMR in δ (ppm): 0.09 (sing. SiCH₃), 7.33–6.39 (mult. 12H, Ar), 4.23 (sing. 4H, OCH₂).

2.5.7. TBC-3

Off-white sticky solid; yield 64%. FT-IR (KBr pellet) in ν (cm⁻¹): 3317 (m, N–H stretch), 3139, 3064 (w, C–H stretch Ar), 2956, 2871 (w, C–H stretch Al), 1711 (s, ester C=O stretch), 1652 (s, amide-I), 1527 (s, amide-II), 1263 (s, Si–CH₃), 1107, 1023 (s, Si–O–Si stretch), 833 (m, C₆H₄ bend). ¹H NMR in δ (ppm) and J (Hz): 0.15 (sing. SiCH₃), 7.42–6.59 (mult. 12H, Ar), 4.24 (trip. 4H, $J = 6.9$, OCH₂), 1.93 (pent. 2H, $J = 7.0$, CH₂).

2.5.8. TBC-4

Off-white sticky solid; yield 62%. FT-IR (KBr pellet) in ν (cm⁻¹): 3321 (m, N–H stretch), 3132, 3057 (w, C–H stretch Ar), 2946, 2869 (w, C–H stretch Al), 1709 (s, ester C=O stretch), 1650 (s, amide-I), 1522 (s, amide-II), 1261 (s, Si–CH₃), 1099, 1022 (s, Si–O–Si stretch), 829 (m, C₆H₄ bend). ¹H NMR in δ (ppm) and J (Hz): 0.14 (sing. SiCH₃), 7.44–6.31 (mult. 12H, Ar), 4.29 (trip. 4H, $J = 7.3$, OCH₂), 1.92 (pent. 4H, $J = 7.3$, CH₂).

2.5.9. TBC-5

Pale sticky solid; yield 65%. FT-IR (KBr pellet) in ν (cm⁻¹): 3308 (m, N–H stretch), 3146, 3063 (w, C–H stretch Ar), 2915, 2866 (w, C–H stretch Al), 1703 (s, ester C=O stretch), 1649 (s, amide-I), 1533 (s, amide-II), 1262 (s, Si–CH₃), 1098, 1014 (s, Si–O–Si stretch), 834 (m, C₆H₄ bend). ¹H NMR in δ (ppm) and J (Hz): 0.16 (sing. SiCH₃), 7.43–6.39 (mult. 12H, Ar), 4.23 (trip. 4H, $J = 7.1$, OCH₂), 1.89–1.53 (mult. 6H, CH₂).

2.5.10. TBC-6

Pale sticky solid; yield 67%. FT-IR (KBr pellet) in ν (cm⁻¹): 3301 (m, N–H stretch), 3163, 3037 (w, C–H stretch Ar), 2933, 2874 (w, C–H stretch Al), 1704 (s, ester C=O stretch), 1650 (s, amide-I), 1538 (s, amide-II), 1264 (s, Si–CH₃), 1107, 1022 (s, Si–O–Si stretch), 833 (m, C₆H₄ bend). ¹H NMR in δ (ppm) and J (Hz): 0.19 (sing. SiCH₃), 7.55–6.34 (mult. 12H, Ar), 4.24 (trip. 4H, $J = 7.3$, OCH₂), 1.94–1.66 (mult. 8H, CH₂).

2.5.11. IBC-2

Off-white sticky solid; yield 61%. FT-IR (KBr pellet) in ν (cm⁻¹): 3298 (m, N–H stretch), 3134, 3055 (w, C–H stretch Ar), 2963, 2858 (w, C–H stretch Al), 1713 (s, ester C=O stretch), 1653 (s, amide-I), 1532 (s, amide-II), 1259 (s, Si–CH₃), 1103, 1025 (s, Si–O–Si stretch), 899, 786, 692 (m, C₆H₄ bend). ¹H NMR in δ (ppm): 0.15 (sing. SiCH₃), 7.54–6.41 (mult. 12H, Ar), 4.23 (sing. 4H, OCH₂).

2.5.12. IBC-3

Off-white sticky solid; yield 60%. FT-IR (KBr pellet) in ν (cm⁻¹): 3305 (m, N–H stretch), 3153, 3062 (w, C–H stretch Ar), 2969, 2856 (w, C–H stretch Al), 1709 (s, ester C=O stretch), 1655 (s, amide-I), 1529 (s, amide-II), 1262 (s, Si–CH₃), 1098, 1017 (s, Si–O–Si stretch), 901, 764, 697 (m, C₆H₄ bend). ¹H NMR in δ (ppm) and J (Hz): 0.16 (sing. SiCH₃), 7.52–6.46 (mult. 12H, Ar), 4.19 (trip. 4H, $J = 6.9$, OCH₂), 1.88 (pent. 2H, $J = 6.8$, CH₂).

2.5.13. IBC-4

Off-white sticky solid; yield 59%. FT-IR (KBr pellet) in ν (cm⁻¹): 3303 (m, N–H stretch), 3161, 3059 (w, C–H stretch Ar), 2939, 2878 (w, C–H stretch Al), 1711 (s, ester C=O stretch), 1652 (s, amide-I), 1529 (s, amide-II), 1262 (s, Si–CH₃), 1101, 1017 (s, Si–O–Si stretch), 905, 797, 695 (m, C₆H₄ bend). ¹H NMR in δ (ppm) and J (Hz): 0.17 (sing. SiCH₃), 7.49–6.33 (mult. 12H, Ar), 4.28 (trip. 4H, $J = 7.0$, OCH₂), 1.81 (pent. 4H, $J = 7.3$, CH₂).

2.5.14. IBC-5

Off-white sticky solid; yield 64%. FT-IR (KBr pellet) in ν (cm⁻¹): 3311 (m, N–H stretch), 3157, 3049 (w, C–H stretch Ar), 2966, 2835 (w, C–H stretch Al), 1707 (s, ester C=O stretch), 1652 (s, amide-I), 1531 (s, amide-II), 1260 (s, Si–CH₃), 1093, 1017 (s, Si–O–Si stretch), 894, 799, 701 (m, C₆H₄ bend). ¹H NMR in δ (ppm) and J (Hz): 0.17 (sing. SiCH₃), 7.49–6.34 (mult. 12H, Ar), 4.27 (trip. 4H, $J = 7.1$, OCH₂), 1.85–1.63 (mult. 6H, CH₂).

2.5.15. IBC-6

Off-white sticky solid; yield 67%. FT-IR (KBr pellet) in ν (cm⁻¹): 3309 (m, N–H stretch), 3167, 3059 (w, C–H stretch Ar), 2943, 2869 (w, C–H stretch Al), 1708 (s, ester C=O stretch), 1651 (s, amide-I), 1529 (s, amide-II), 1263 (s, Si–CH₃), 1097, 1016 (s, Si–O–Si stretch), 889, 801, 706 (m, C₆H₄ bend). ¹H NMR in δ (ppm) and J (Hz): 0.19 (sing. SiCH₃), 7.51–6.36 (mult. 12H, Ar), 4.26 (trip. 4H, $J = 6.9$, OCH₂), 1.93–1.57 (mult. 8H, CH₂).

2.6. Synthesis of polyesteramides

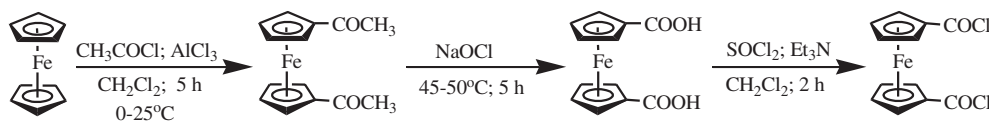
The corresponding polyesteramides of the synthesized block copolymers, without polydimethylsiloxane (PDMS) segment, were prepared under similar conditions. In a two-necked pre-baked flask, the corresponding diamine (1.84 mmol) was dissolved in freshly dried hot THF (15 ml) and treated with triethylamine (10 ml) under an inert atmosphere. The temperature was lowered to 0 °C using an ice bath and 1,1'-ferrocenedicarbonyl chloride (0.600 g, 1.92 mmol) dissolved in dry THF (10 ml) was added drop-wise with vigorous stirring over a period of 30 min. The temperature was slowly raised to room temperature and the mixture was stirred for 1 h and then allowed to reflux for an additional hour. The precipitated product was then collected by filtration, washed with THF (3 × 5 ml) and several times with methanol. The resulting product was dried in vacuum for 24 h. The organic analogues of the polyesteramides were prepared by similar procedure using terephthaloyl chloride and isophthaloyl chloride. Synthesis of these polyamides is summarized in [Scheme 4](#).

2.6.1. FcA-2

Reddish brown solid; yield 86%. FT-IR (KBr pellet) in ν (cm⁻¹): 3316 (m, N–H stretch), 3098, 3032 (w, C–H stretch Ar), 2927, 2846 (w, C–H stretch Al), 1712 (s, ester C=O stretch), 1654 (s, amide-I), 1523 (s, amide-II), 823 (m, C₆H₄ bend), 490 (m, Fe–Cp). ¹H NMR in δ (ppm): 5.08–4.53 (br. 8H, Cp), 7.64–6.53 (mult. 8H, Ar), 4.18 (sing. 4H, OCH₂).

2.6.2. FcA-3

Reddish brown solid; yield 88%. FT-IR (KBr pellet) in ν (cm⁻¹): 3328 (m, N–H stretch), 3130, 3053 (w, C–H stretch Ar), 2944, 2821



Scheme 1. Synthesis of ferrocene monomer (1,1'-ferrocenedicarbonyl chloride).

(w, C–H stretch Al), 1709 (s, ester C=O stretch), 1653 (s, amide-I), 1534 (s, amide-II), 828 (m, C₆H₄ bend), 493 (m, Fe–Cp). ¹H NMR in δ (ppm) and J (Hz): 5.03–4.46 (br. 8H, Cp), 7.61–6.53 (mult. 8H, Ar), 4.11 (trip. 4H, $J = 7.2$, OCH₂), 2.01 (pent. 2H, $J = 7.3$, CH₂).

2.6.3. FcA-4

Brown solid; yield 90%. FT-IR (KBr pellet) in ν (cm⁻¹): 3317 (m, N–H stretch), 3123, 3042 (w, C–H stretch Ar), 2943, 2887 (w, C–H stretch Al), 1707 (s, ester C=O stretch), 1654 (s, amide-I), 1519 (s, amide-II), 835 (m, C₆H₄ bend), 498 (m, Fe–Cp). ¹H NMR in δ (ppm) and J (Hz): 5.07–4.49 (br. 8H, Cp), 7.67–6.60 (mult. 8H, Ar), 4.19 (trip. 4H, $J = 6.9$, OCH₂), 1.97 (pent. 4H, $J = 7.7$, CH₂).

2.6.4. FcA-5

Dark brown solid; yield 91%. FT-IR (KBr pellet) in ν (cm⁻¹): 3339 (m, N–H stretch), 3119, 3072 (w, C–H stretch Ar), 2923, 2852 (w, C–H stretch Al), 1711 (s, ester C=O stretch), 1651 (s, amide-I), 1529 (s, amide-II), 834 (m, C₆H₄ bend), 501 (m, Fe–Cp). ¹H NMR in δ (ppm) and J (Hz): 5.03–4.51 (br. 8H, Cp), 7.69–6.54 (mult. 8H, Ar), 4.21 (trip. 4H, $J = 6.9$, OCH₂), 1.71–1.49 (mult. 6H, CH₂).

2.6.5. FcA-6

Dark brown solid; yield 93%. FT-IR (KBr pellet) in ν (cm⁻¹): 3327 (m, N–H stretch), 3124, 3047 (w, C–H stretch Ar), 2924, 2855 (w,

C–H stretch Al), 1708 (s, ester C=O stretch), 1651 (s, amide-I), 1518 (s, amide-II), 826 (m, C₆H₄ bend), 497 (m, Fe–Cp). ¹H NMR in δ (ppm) and J (Hz): 4.99–4.50 (br. 8H, Cp), 7.71–6.66 (mult. 8H, Ar), 4.21 (trip. 4H, $J = 7.3$, OCH₂), 1.78–1.68 (mult. 8H, CH₂).

2.6.6. TA-2

White solid; yield 87%. FT-IR (KBr pellet) in ν (cm⁻¹): 3349 (m, N–H stretch), 3115, 3084 (w, C–H stretch Ar), 2931, 2877 (w, C–H stretch Al), 1704 (s, ester C=O stretch), 1646 (s, amide-I), 1531 (s, amide-II), 837 (m, C₆H₄ bend). ¹H NMR in δ (ppm): 7.74–6.62 (mult. 12H, Ar), 4.11 (sing. 4H, OCH₂).

2.6.7. TA-3

White solid; yield 86%. FT-IR (KBr pellet) in ν (cm⁻¹): 3335 (m, N–H stretch), 3118, 3077 (w, C–H stretch Ar), 2922, 2852 (w, C–H stretch Al), 1707 (s, ester C=O stretch), 1650 (s, amide-I), 1531 (s, amide-II), 803 (m, C₆H₄ bend). ¹H NMR in δ (ppm) and J (Hz): 7.68–6.42 (mult. 12H, Ar), 4.22 (trip. 4H, $J = 7.1$, OCH₂), 1.97 (pent. 2H, $J = 7.0$, CH₂).

2.6.8. TA-4

Off-white solid; yield 89%. FT-IR (KBr pellet) in ν (cm⁻¹): 3321 (m, N–H stretch), 3117, 3081 (w, C–H stretch Ar), 2931, 2847 (w, C–H stretch Al), 1702 (s, ester C=O stretch), 1649 (s, amide-I), 1527 (s, amide-II), 817 (m, C₆H₄ bend). ¹H NMR in δ (ppm) and J (Hz): 7.79–6.56 (mult. 12H, Ar), 4.23 (trip. 4H, $J = 7.1$, OCH₂), 1.93 (pent. 4H, $J = 7.5$, CH₂).

2.6.9. TA-5

Pale solid; yield 90%. FT-IR (KBr pellet) in ν (cm⁻¹): 3314 (m, N–H stretch), 3128, 3076 (w, C–H stretch Ar), 2937, 2858 (w, C–H stretch Al), 1704 (s, ester C=O stretch), 1643 (s, amide-I), 1523 (s, amide-II), 821 (m, C₆H₄ bend). ¹H NMR in δ (ppm) and J (Hz): 7.71–6.56 (mult. 12H, Ar), 4.19 (trip. 4H, $J = 7.1$, OCH₂), 1.72–1.51 (mult. 6H, CH₂).

2.6.10. TA-6

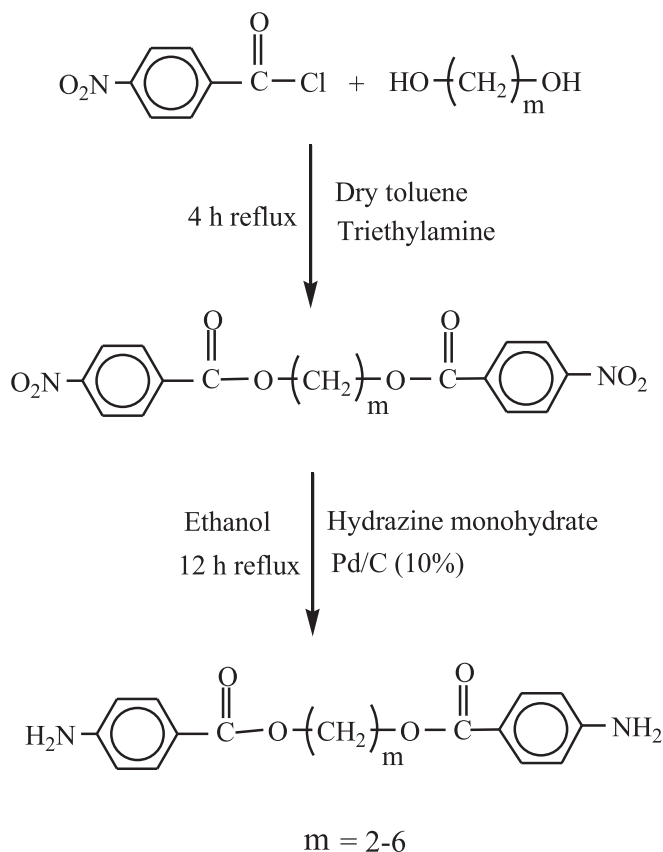
Off-white solid; yield 92%. FT-IR (KBr pellet) in ν (cm⁻¹): 3319 (m, N–H stretch), 3123, 3038 (w, C–H stretch Ar), 2929, 2856 (w, C–H stretch Al), 1699 (s, ester C=O stretch), 1643 (s, amide-I), 1528 (s, amide-II), 827 (m, C₆H₄ bend). ¹H NMR in δ (ppm) and J (Hz): 7.78–6.63 (mult. 12H, Ar), 4.26 (trip. 4H, $J = 7.3$, OCH₂), 1.73–1.49 (mult. 8H, CH₂).

2.6.11. IA-2

White solid; yield 87%. FT-IR (KBr pellet) in ν (cm⁻¹): 3321 (m, N–H stretch), 3121, 3049 (w, C–H stretch Ar), 2933, 2857 (w, C–H stretch Al), 1714 (s, ester C=O stretch), 1654 (s, amide-I), 1519 (s, amide-II), 884, 809, 723 (m, C₆H₄ bend). ¹H NMR in δ (ppm): 7.56–6.61 (mult. 12H, Ar), 4.22 (sing. 4H, OCH₂).

2.6.12. IA-3

Off-white solid; yield 86%. FT-IR (KBr pellet) in ν (cm⁻¹): 3329 (m, N–H stretch), 3113, 3044 (w, C–H stretch Ar), 2962, 2852 (w, C–H stretch Al), 1712 (s, ester C=O stretch), 1652 (s, amide-I), 1531 (s, amide-II), 897, 765, 692 (m, C₆H₄ bend). ¹H NMR in δ (ppm) and J (Hz): 7.71–6.59 (mult. 12H, Ar), 4.19 (trip. 4H, $J = 6.9$, OCH₂), 1.98 (pent. 2H, $J = 6.8$, CH₂).



Scheme 2. Synthesis of organic diamine monomers.

2.6.13. IA-4

Off-white solid; yield 89%. FT-IR (KBr pellet) in ν (cm^{-1}): 3323 (m, N–H stretch), 3119, 3047 (w, C–H stretch Ar), 2941, 2856 (w, C–H stretch Al), 1713 (s, ester C=O stretch), 1653 (s, amide-I), 1518 (s, amide-II), 892, 779, 701 (m, C_6H_4 bend). ^1H NMR in δ (ppm) and J (Hz): 7.72–6.67 (mult. 12H, Ar), 4.23 (trip. 4H, $J = 7.3$, OCH_2), 1.99 (pent. 4H, $J = 7.1$, CH_2).

2.6.14. IA-5

Pale solid; yield 92%. FT-IR (KBr pellet) in ν (cm^{-1}): 3326 (m, N–H stretch), 3113, 3056 (w, C–H stretch Ar), 2937, 2856 (w, C–H stretch Al), 1711 (s, ester C=O stretch), 1651 (s, amide-I), 1524 (s, amide-II), 897, 778, 699 (m, C_6H_4 bend). ^1H NMR in δ (ppm) and J (Hz): 7.69–6.53 (mult. 12H, Ar), 4.24 (trip. 4H, $J = 6.9$, OCH_2), 1.67–1.58 (mult. 6H, CH_2).

2.6.15. IA-6

Off-white solid; yield 91%. FT-IR (KBr pellet) in ν (cm^{-1}): 3325 (m, N–H stretch), 3116, 3064 (w, C–H stretch Ar), 2925, 2854 (w, C–H stretch Al), 1713 (s, ester C=O stretch), 1651 (s, amide-I), 1527 (s, amide-II), 851, 766, 693 (m, C_6H_4 bend). ^1H NMR in δ (ppm) and J (Hz): 7.34–6.51 (mult. 12H, Ar), 4.18 (trip. 4H, $J = 7.2$, OCH_2), 1.69–1.61 (mult. 8H, CH_2).

Stretch = stretching, bend = bending, m = medium, s = sharp, w = weak, Al = aliphatic, Ar = aromatic, br. = broad, sing. = singlet, doub. = doublet, trip. = triplet, pent. = pentet, mult. = multiplet.

3. Results and discussion

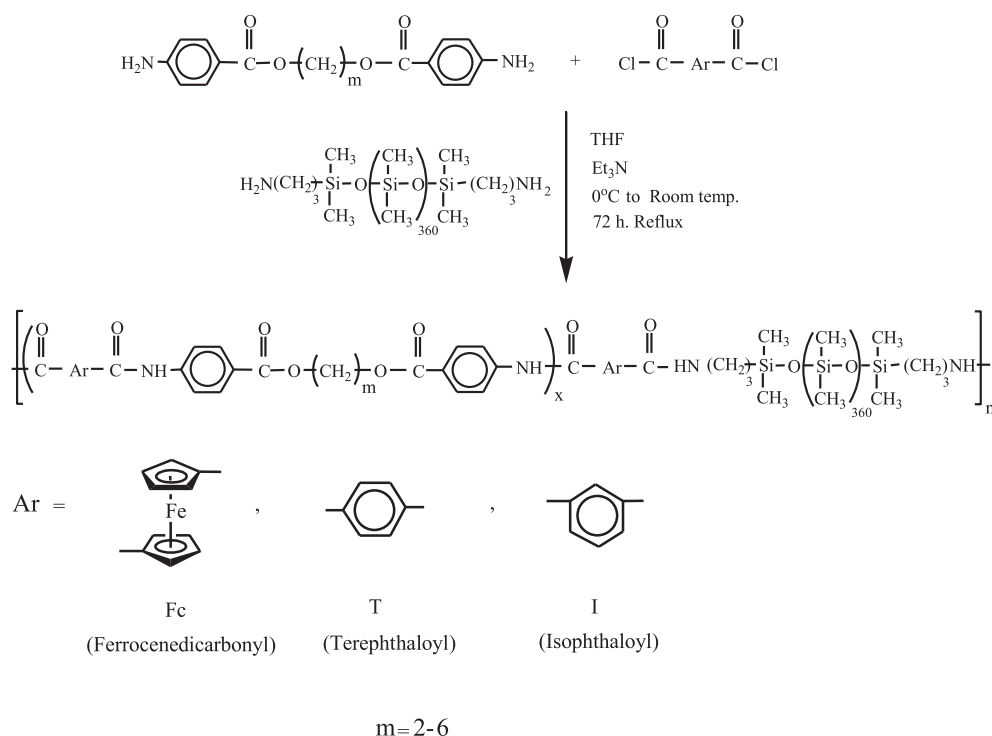
3.1. Monomer synthesis and characterization

The ferrocene-based monomer, 1,1'-ferrocene dicarbonyl chloride was prepared from ferrocene in three steps by an improved and efficient method (Scheme 1) [34]. The diamine monomers, bis(ester-amine)s, with variable aliphatic character and pre-formed

ester linkages were synthesized in two steps (Scheme 2). The dinitro-diester of the general formula 1,*m*-bis(4-nitrobenzoyloxy) alkanes ($m = 2-6$), were prepared in good yields in the first step by nucleophilic substitution reactions under an inert atmosphere using Schotten–Baumann conditions [36]. The reaction occurred immediately at low temperature (10°C) as precipitated $\text{Et}_3\text{N-HCl}$ (derived from hydrochloric acid produced in the reaction and triethyl amine) was observed as soon as the solution of 4-nitrobenzoyl chloride in reaction solvent was added drop-wise to the reaction flask. The low temperature conditions were required to prevent the hydrolysis of the ester group (O=C-O). It was also observed that the replacement of the toluene reaction solvent with THF had no marked effect upon reaction times or yields of the final products.

The synthesized dinitro precursors were then reduced in the second step to the corresponding semi-aromatic diamine compounds, 1,*m*-bis(4-aminobenzoyloxy)alkanes ($m = 2-6$) using hydrazine monohydrate as reducing agent. The solution of hydrazine hydrate in ethanol (1:2) was added drop-wise over half an hour to the suspension of dinitro species and Pd–C catalyst in refluxing ethanol in order to avoid the hydrazinolysis of the ester group during reduction. The reaction mixture was then evaporated on a rotary vacuum evaporator to afford the diamine monomer, which was washed thoroughly with distilled water to remove the traces of hydrazine.

The synthesized dinitro precursors (N-2, N-3, N-4, N-5 and N-6) and the diamine monomers (D-2, D-3, D-4, D-5 and D-6) were purified by recrystallization in ethanol and their purity were checked by TLC in *n*-hexane and ethyl acetate (1:1) mixture. The dinitro-diester were yellow while the diamine monomers were white in colour. All these compounds were soluble in common organic solvents (ethanol, chloroform, toluene, etc.) and possessed sharp melting points. The observed values for carbon, hydrogen and nitrogen of the intermediates and the resulting monomers were in good agreement with the calculated ones.



Scheme 3. Synthesis of block copolymers of ferrocene-based polyesteramides and their organic analogues with polydimethylsiloxane (PDMS).

The FTIR spectra of all the dinitro precursors exhibited two characteristic nitro group bands at 1527–1522 cm^{-1} (asymmetrical stretching) and 1356–1349 cm^{-1} (symmetrical stretching) respectively. The ester group was characterized by a sharp absorption band at 1726–1718 cm^{-1} . The aromatic and aliphatic moieties in the compounds were identified by the bands at 3117–3110 cm^{-1} , 3094–3078 cm^{-1} (aromatic C–H stretching) and 2969–2933 cm^{-1} , 2870–2854 cm^{-1} (aliphatic C–H stretching) in each spectrum. After reduction, the disappearance of nitro bands indicated a virtually complete conversion of dinitro functionality to diamine. Moreover, the spectra of synthesized diamines also contained a typical N–H stretching absorption pair at 3465–3394 cm^{-1} and 3374–3336 cm^{-1} . The presence of a sharp band (1694–1674 cm^{-1}) in each spectrum shows that the carbonyl ester group is intact in the synthesized diamines. The shifting of bands to lower wave numbers compared to those present in dinitro compounds is due to the electron donating effect of NH_2 group [36,37]. The spectra also contained the bands due to the aromatic and aliphatic moieties.

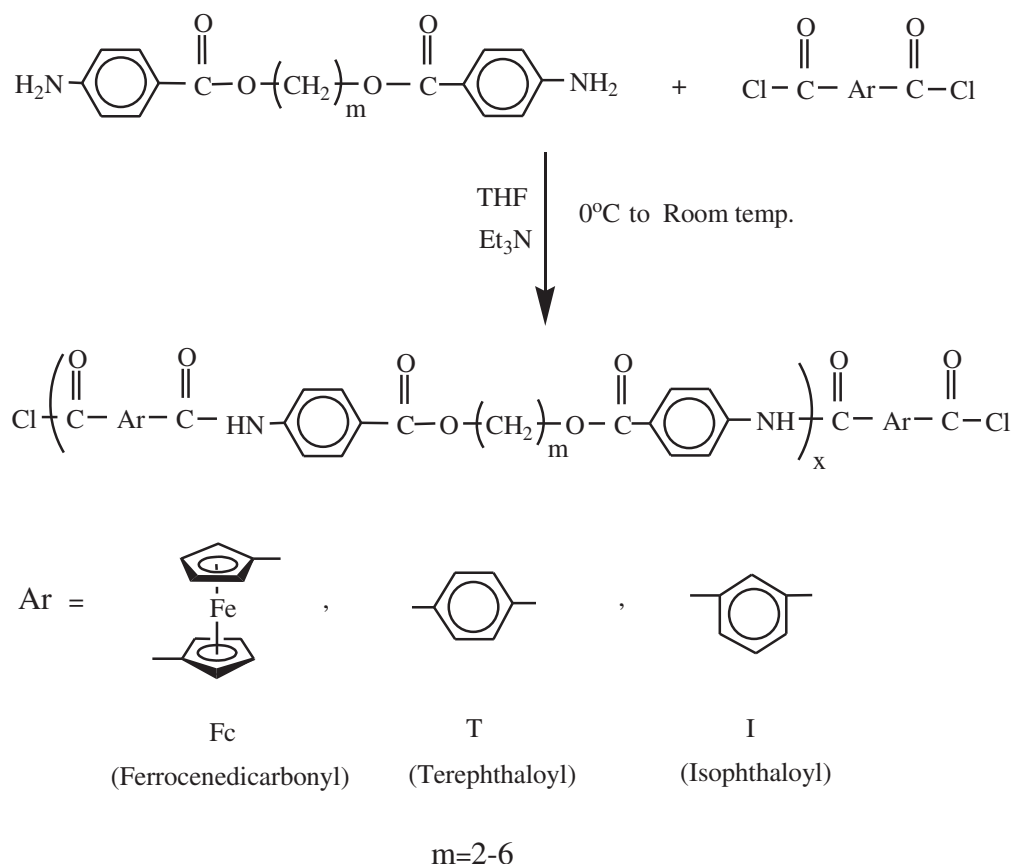
The ^1H NMR spectra of the synthesized dinitro compounds were also consistent with the proposed molecular structures. The signals associated with different aromatic and aliphatic protons could be observed in each spectrum. The aromatic protons in proximity to NO_2 groups resonated farthest downfield due to the deshielding effect of the electron-withdrawing nitro groups [37]. The appearance of characteristic signals at ca. 5.9 ppm corresponding to the amino protons in the spectra of diamine monomers and the upfield chemical shift of the aromatic protons due to the electron donating ability of the amino group [36,37] confirmed the conversion of nitro groups into the amino functionalities.

The ^{13}C NMR spectra of the dinitro intermediates and synthesized diamines also exhibited the signals due to the presence of aromatic and methylene carbons. The presence of the ester group in each compound was evident from the characteristic farthest downfield signals (ca. 166 ppm) attributable to the carbonyl carbon of the ester group.

The different dinitro intermediates and the diamines vary in the number of methylene spacers. The intensities of the bands associated with the aliphatic moieties in the FTIR spectra changed with the change in number of methylene spacers [36,37]. Moreover, the number and integration of aliphatic protons were different in the ^1H NMR spectra of the different dinitro intermediates and the diamine monomers. The difference in methylene spacers was also exhibited in the ^{13}C NMR spectra by different number of signals. The representative FTIR, ^1H NMR and ^{13}C NMR spectra of the dinitro precursors and related diamine monomers are presented as [Supplementary material](#).

3.2. Synthesis of block copolymers and their corresponding polyesteramides

The block copolymers of structurally modified ferrocene-based organometallic polyesteramides as well as their organic analogues with aminopropyl-terminated polydimethylsiloxane (PDMS) oligomer were synthesized by a one-pot two-step solution polycondensation procedure in THF under inert conditions (Scheme 3). The reaction did not proceed even after one week (168 h) reflux and both reagents could be isolated when the polyesteramides were synthesized separately and utilized for copolymerization with PDMS, due to the conversion of terminal chloride functionalities



Scheme 4. Synthesis of corresponding organometallic and organic polyesteramides without polydimethylsiloxane (PDMS) segment.

and ^1H NMR spectroscopic studies and the molar masses were determined by static laser light scattering technique.

The FT-IR spectra of the block copolymers provided evidence for the presence of all expected functional groups in their backbone. The spectra exhibited $-\text{NH}$ stretching frequencies in the range $3321\text{--}3293\text{ cm}^{-1}$, amide-I bands (associated with the stretching vibration of the carbonyl group [42]) in the range $1654\text{--}1647\text{ cm}^{-1}$ and amide-II absorption bands [42] (ascribed to the coupling of the N–H bending and C–N stretching of the C–N–H group) in the range $1539\text{--}1522\text{ cm}^{-1}$ along with the bands attributed to the presence of aromatic and aliphatic moieties. The presence of ester group in the synthesized copolymers could also be identified in the respective spectra by a sharp absorption band at $1713\text{--}1703\text{ cm}^{-1}$. In addition, the spectra also exhibited prominent peaks at *ca.* 1262 cm^{-1} due to symmetrical $\text{CH}_3\text{--Si}$ deformation modes and a doublet with maxima at *ca.* $1107\text{--}1093\text{ cm}^{-1}$ and $1025\text{--}1014\text{ cm}^{-1}$

attributed to Si–O–Si asymmetric stretch, which confirmed the incorporation of PDMS moiety in all these copolymers [26,39]. It is reported that an isolated Si–O–Si group gives a single broad band near 1050 cm^{-1} [26,39]. The precise position of this band depends on the inductive, steric and mass effects of the substituents. The disubstituted linear siloxane oligomers, on the other hand, exhibit Si–O–Si absorption for each unit in the chains, but these bands overlap and develop a broad doublet pattern with absorption maxima at 1090 and 1020 cm^{-1} , when the number of coupled siloxane units becomes greater than 20 [26,39]. The distinguishing feature of the spectra of ferrocene-containing organometallic copolymers was the presence of a medium intensity Fe–Cp stretching band in the range $503\text{--}495\text{ cm}^{-1}$, which was absent in the spectra of the organic copolymers. It was observed that there exists a remarkable similarity among the spectra of the organometallic and organic copolymers except for the bands associated with aliphatic

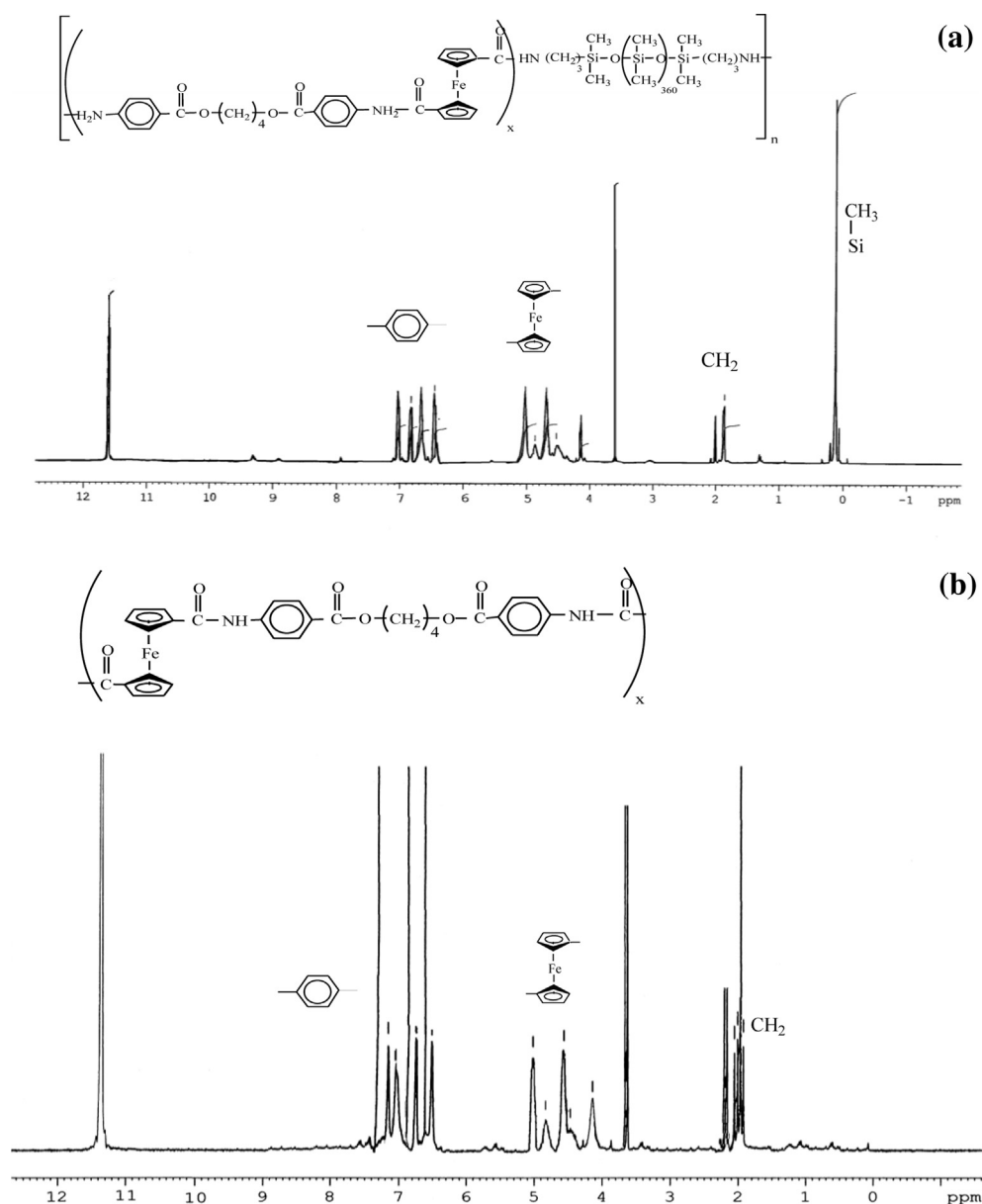


Fig. 2. ^1H NMR spectra of the synthesized copolymer FcBC-4 (a) and corresponding polyesteramide FcA-4 (b).

Table 1
Static laser light-scattering results of the synthesized copolymers^a in toluene at 25 °C.

Polymer	$M_w \times 10^{-5}$ (g mol ⁻¹)	$\langle R_g \rangle$ (nm)	A_2 (cm ³ mol g ⁻²)
FcBC-2	6.32	43	3.57×10^{-4}
FcBC-3	5.13	46	1.37×10^{-4}
FcBC-4	9.08	55	3.44×10^{-4}
FcBC-5	1.66	33	2.50×10^{-4}
FcBC-6	8.76	31	5.90×10^{-4}
TBC-2	5.96	51	4.39×10^{-4}
TBC-3	4.84	39	3.76×10^{-4}
TBC-4	4.17	57	6.12×10^{-4}
TBC-5	3.80	34	5.10×10^{-4}
TBC-6	9.39	38	4.39×10^{-4}
IBC-2	4.42	44	5.37×10^{-4}
IBC-3	6.63	48	1.93×10^{-4}
IBC-4	7.33	37	5.25×10^{-4}
IBC-5	5.89	52	5.77×10^{-4}
IBC-6	7.05	36	4.86×10^{-4}

The relative errors are: dn/dc , $\pm 1\%$; M_w , $\pm 5\%$; $\langle R_g \rangle$ and A_2 , $\pm 10\%$.

^a The data presented are for the N-trifluoroacetylated polymer species.

and aromatic C–H groups, which change essentially according to the change in orientation (para or meta) and number of methylene spacers. The FTIR spectrum of synthesized copolymer FcBC-5, as an example, is shown in Fig. 1(a).

The FTIR spectra of the corresponding polyesteramides contained strong absorption bands in the region 1714–1702 cm⁻¹ due to the presence of ester groups [43] along with the amide-I and amide-II bands. The –NH stretching frequency bands in these polymers were present at ca. 3367–3314 cm⁻¹. The distinctive feature of these bands was a shoulder in each spectrum in the range 3411–3376 cm⁻¹. The existence of the –NH bands with overlaying shoulders indicates that more than one type of hydrogen bonding with different bond distances for N–H group is present in these polymers. This observation is in accord with the hydrogen-bonded polyesteramides reported in the literature [43,44].

The ferrocene entities in the organometallic polyesteramides could be ascertained by the presence of a medium intensity Fe–Cp stretching band in the range 501–490 cm⁻¹, which was absent in the spectra of the organic polyesteramides. The terephthaloyl-based polyesteramides exhibited lower amide-I carbonyl absorption frequencies in their spectra (1650–1643 cm⁻¹) compared to the isophthaloyl-based organic and ferrocene-containing organometallic analogues (1654–1651 cm⁻¹). It is believed that hydrogen bonding is the major factor contributing to the lower carbonyl

Table 2
Static laser light-scattering results of the corresponding polyesteramides³ in toluene at 25 °C.

Polymer	$M_w \times 10^{-4}$ (g mol ⁻¹)	$\langle R_g \rangle$ (nm)	A_2 (cm ³ mol g ⁻²)
FcA-2	3.92	30	5.87×10^{-4}
FcA-3	4.17	33	2.14×10^{-4}
FcA-4	4.68	29	8.34×10^{-3}
FcA-5	4.94	24	1.62×10^{-4}
FcA-6	6.73	38	7.27×10^{-4}
TA-2	3.86	25	5.15×10^{-4}
TA-3	4.02	28	4.76×10^{-4}
TA-4	5.12	21	6.93×10^{-4}
TA-5	5.58	32	4.28×10^{-4}
TA-6	3.39	23	8.13×10^{-3}
IA-2	4.42	22	3.64×10^{-4}
IA-3	4.64	27	2.77×10^{-4}
IA-4	6.21	34	9.33×10^{-3}
IA-5	5.19	33	3.42×10^{-4}
IA-6	6.55	31	2.31×10^{-4}

The relative errors are: dn/dc , $\pm 1\%$; M_w , $\pm 5\%$; $\langle R_g \rangle$ and A_2 , $\pm 10\%$.

^a The data presented are for the N-trifluoroacetylated polymer species.

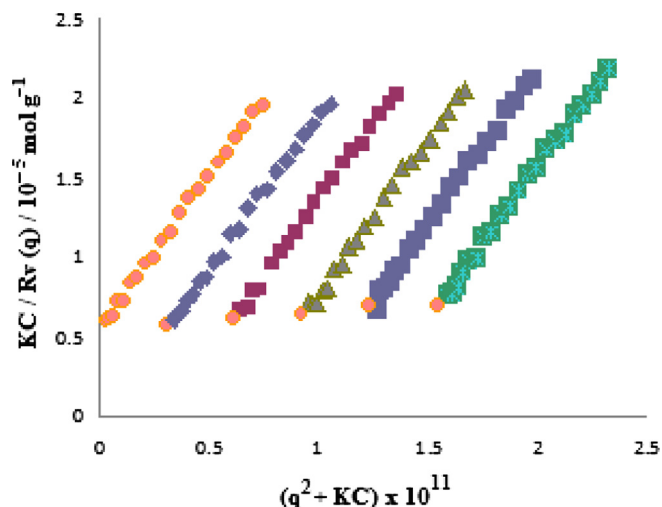


Fig. 3. Representative Zimm plot of the synthesized copolymer FcBC-5.

absorption frequency of the ordered amide-based polymers when they are examined in the solid state [43,44]. The spectra of polyesteramides also exhibited very similar features with the exception that the intensities of bands associated with aliphatic and aromatic C–H groups were different due to changes in orientation (para or meta) and number of methylene spacers as observed in the synthesized copolymers. A representative FTIR spectrum (polyesteramide FcA-5) is given in Fig. 1(b).

The chain structure of the synthesized copolymers was further confirmed by their ¹H NMR spectroscopic studies. The ¹H NMR spectra of the synthesized copolymers were recorded in THF-*d*₈ after trifluoroacetylation without internal standard (tetramethylsilane, TMS), which would interfere with Si–CH₃ signal. The spectra displayed the most remarkable signal corresponding to PDMS segment at ca. 0.0 ppm. All the signals attributed to the aromatic as well as aliphatic protons present in the polyesteramide component could also be identified in the spectra but their intensity was lower relative to the sharp signal of SiCH₃ protons indicating a smaller mass ratio of hard polyesteramide components in the synthesized copolymers compared to the soft PDMS segments. The comparison of the peak area due to the silicon methyl protons with the peak area resulting from the aromatic protons gave the relative composition of the two blocks and suggested that the soft siloxane component has been incorporated to slightly less than the calculated amount in all the synthesized copolymers. The presence of the ferrocene moiety in the organometallic copolymers was affirmed by the characteristic broad resonance signals in the region 5.11–4.47 ppm. This signal broadening indicates the presence of paramagnetic impurities as a result of oxidation of ferrocene to ferrocenium ion [45,46]. The signals attributed to the amide protons were absent in the spectra because of the fact that acetylation

Table 3
Water absorption studies of the representative copolymers and their respective polyesteramides.^a

Copolymer	Water absorption (%)	Polyesteramide	Water absorption (%)
FcBC-2	0.96	FcA-2	5.91
FcBC-6	0.99	FcA-6	5.95
TBC-2	0.94	TA-2	5.92
TBC-6	0.98	TA-6	5.99
IBC-2	0.89	IA-2	6.15
IBC-6	0.87	IA-6	7.05

^a Moisture absorption (%) = $((W_f - W_o)/W_o) \times 100$.

occurs on the nitrogen of the amide bond and eliminates the amide proton, which subsequently adds to the trifluorocarboxylate ion yielding trifluoroacetic acid [47]. Therefore, a signal at ca. 11.5 ppm was observed in the spectra.

The spectra of the related polyesteramides displayed all the characteristic signals of the aromatic as well as aliphatic protons anticipated for their constitution. The difference in the spectra of the organometallic polymers compared to their organic analogues was the presence of the characteristic chemical shifts of Cp protons in the range 5.08–4.46 ppm. Exemplary ^1H NMR spectra of the synthesized copolymer (FcBC-4) and the corresponding polyesteramide (FcA-4) are presented in Figs. 2(a) and (b) respectively.

3.4. Laser light-scattering results

The molecular parameters of the synthesized copolymers were determined in toluene at 25 °C by static laser light scattering (LLS) after N-trifluoroacetylation. Static laser light scattering measures light intensity as a function of scattering angle and solute concentration, and the relationship between the light scattering from a dilute polymer solution and the weight-average molecular weight

can be described by the Zimm formalism [48]. This allows the determination of weight-average molar mass, radius of gyration and shape information of the solute [49]. The molecular parameters of the synthesized copolymers are given in Tables 1 and 2 and representative Zimm plot (FcBC-5) is shown in Fig. 3. The weight-average molar masses of the organometallic copolymers are in the range 1.66×10^5 to $9.08 \times 10^5 \text{ g mol}^{-1}$, which is due to the flexible high molar mass polydimethylsiloxane segment present in the copolymer backbone and comparable with those reported for the siloxane copolymers based on the polyamides containing trichlorogermyl pendant groups [39]. The molar masses of the organic analogues prepared under similar conditions also lie in the same range (3.80×10^5 to $9.39 \times 10^5 \text{ g mol}^{-1}$), indicating that the method used for the synthesis is equally suitable for ferrocene-based organometallic copolymers as well as their organic analogues. The high values also suggest that the synthesized materials are multiblock copolymers [50]. In addition, the values for the radius of gyration $\langle R_g \rangle$ are also slightly high compared to the corresponding organometallic polyesteramides, reflecting the long chain lengths of these copolymers [39,51]. The positive values of the second virial coefficient reflect a very strong polymer–solvent interaction [51]

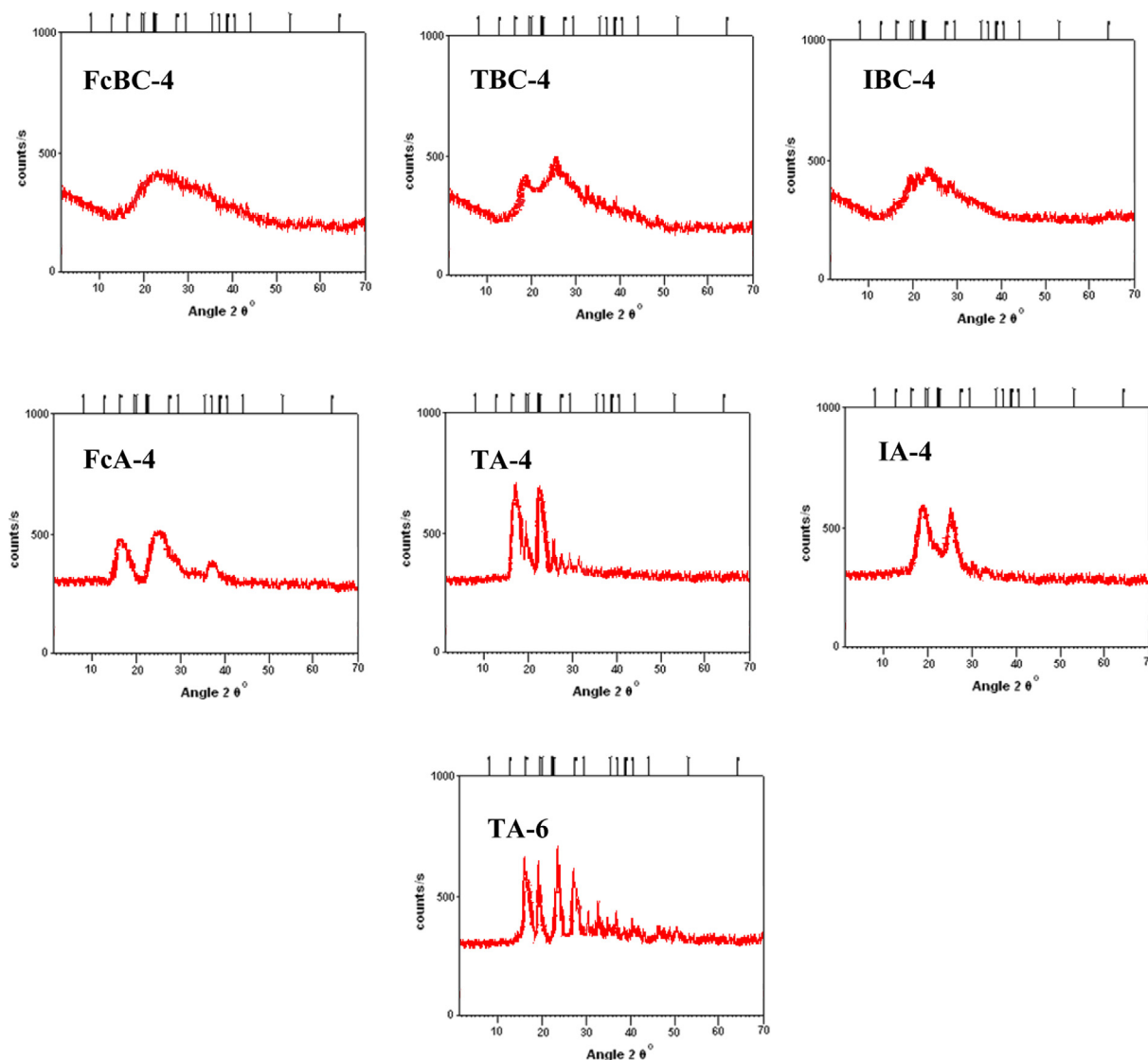


Fig. 4. Wide-angle X-ray diffractograms of some selected polymeric materials surface morphology.

indicating that N-trifluoroacetylation is an effective way to disrupt the intermolecular interactions between the polymer chains which allows the subsequent penetration of solvent molecules to these structures.

The weight-average molar masses of the respective organometallic polyesteramides and their organic analogues lie between 33,900 and 67,300 g mol⁻¹. The radius of gyration (R_g) values of these polymers were in the range 21–38 nm and the second virial coefficient values also indicated a very strong polymer–solvent interaction upon trifluoroacetylation.

3.5. Solubility behaviour

The solubility behaviour of the synthesized block copolymers was tested qualitatively. All the polymeric materials were found insoluble or slightly soluble in common organic solvents such as chloroform, dichloromethane, etc. The insolubility may be attributed to the chain stiffness caused by the inherent rigidity of the amide linkage present in the copolymers as well as the intermolecular dipole–dipole and hydrogen bonding interactions between the chains [52,53], and in part to the increase in molecular weights on incorporation of the polydimethylsiloxane unit in the polymers as the solubility decreases with the increase in molecular weight [54]. The introduction of flexible methylene spacers along with ester linkages which are generally recognized to enhance solubility [8] did not prove greatly effective in breaking the intermolecular interactions in the synthesized copolymers. It has been reported that sometimes these flexible linkages play only a minor role in solubility, their influence being subordinate to other groups in the polymer chain [55]. The synthesized copolymers, however, were partially soluble in polar aprotic solvents such as DMF and DMSO. The limited solubility in polar aprotic solvents reveals the partial ability of these solvents to overcome the intermolecular interactions. The solubility was also tested in mixtures of solvents. The solvent system containing toluene and THF (1:1) was effective on heating to solubilize the synthesized copolymers but the solubility decreased on cooling to room temperature. All the synthesized copolymers were found to be soluble in conc. H₂SO₄ and

could be precipitated with methanol, water, etc. It is believed that H₂SO₄ protonates the nitrogen of the amide group to overcome the hydrogen bonding forces, thus solubilizing the polymers [52,54].

The corresponding organometallic as well as the organic polyesteramides also exhibited limited solubility in organic solvents due to the rigid amide groups and hydrogen bonding in them [52,53], and were found to be soluble in conc. H₂SO₄, as was the case for their respective copolymers.

The synthesized copolymers and their polyesteramide counterparts could be solubilized in common organic solvents upon trifluoroacetylation using trifluoroacetic anhydride (TFAA) as reported in the literature [47,56]. Acetylation occurs on the nitrogen of the amide bond and disrupts the hydrogen bonding to solubilize the materials in the solvent medium [47]. All the synthesized organometallic and organic copolymers could be trifluoroacetylated readily and become solubilized when a few drops of TFAA are added to the stirred suspension of the copolymer in the solvent (THF, CHCl₃, etc.) at 0 °C. It was also observed that the ferrocene-based organometallic polyamides and their isophthaloyl-based analogues can be trifluoroacetylated easily and become soluble in the common organic solvents upon 1–2 h stirring, compared to the terephthaloyl-based polymers, which solubilize only after stirring overnight (12 h). This behaviour may be attributed to the crystalline nature of terephthaloyl-based polymers [57] in which the polymer chains are highly ordered and densely packed rendering disruption of inter-chain hydrogen bonding more difficult. The low solubility of these polymeric and copolymeric materials suggests their utilization in applications where extreme solvent resistance is required.

3.6. Water absorption studies

The water absorption studies of some representative copolymers and their respective polyesteramides were carried out following the ASTM D570-81 procedure [31]. The results obtained for these studies are listed in Table 3. The results show that all the synthesized copolymers absorbed very little water (ca. 1%), in contrast to their polyesteramide counterparts which absorbed

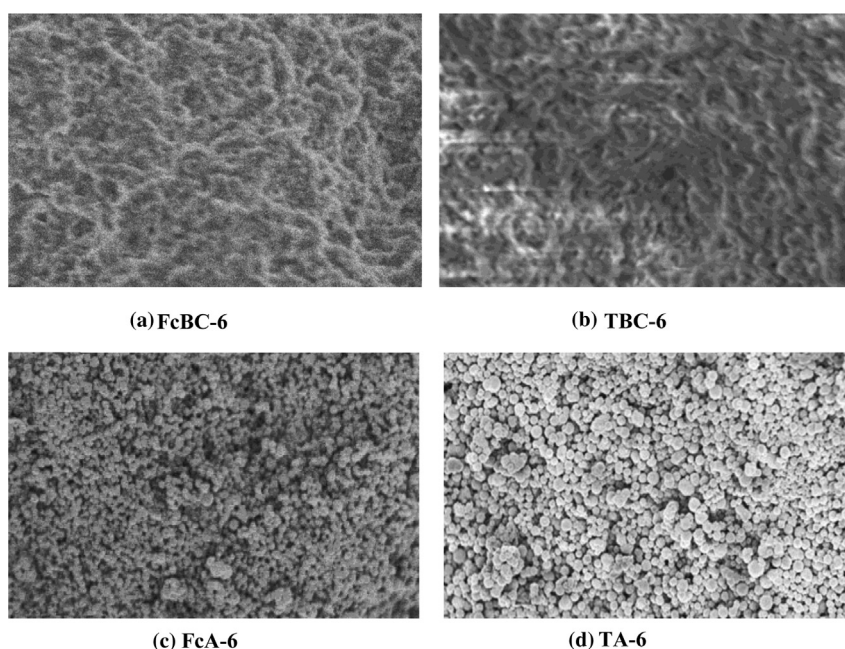


Fig. 5. Representative scanning electron micrographs of the synthesized block copolymers and their respective polyesteramide.

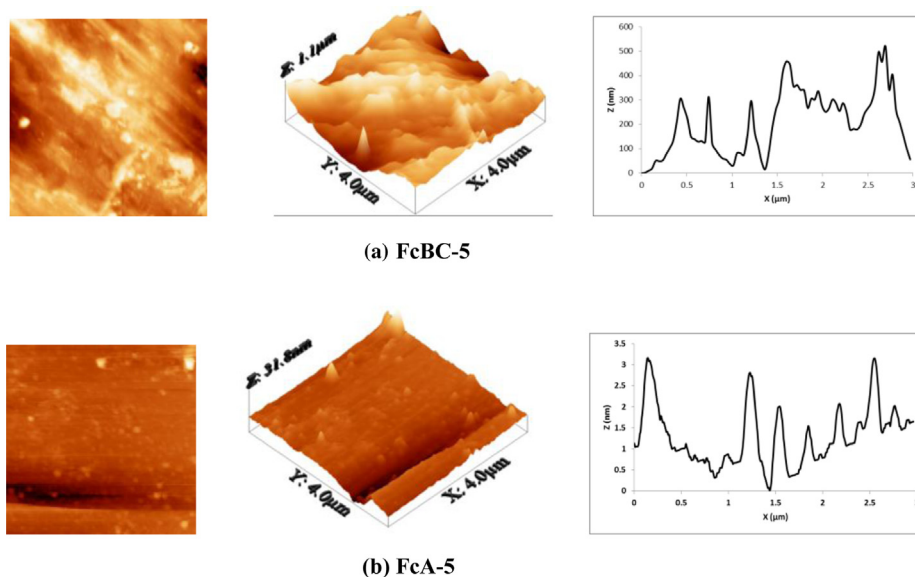


Fig. 6. Representative AFM topographic images and roughness profile graphs of the synthesized block copolymers and their corresponding polyesteramide.

water in the range 5.95–7.05%. The water absorption of polyesteramides is attributed to the abundance of polar ester and amide groups exposed on the polymer surface where water molecules develop secondary interactions with these groups [58], and can adversely affect their mechanical and dielectric properties [58,59]. However, the hydrophilic nature makes the polyesteramides good candidates for semi-permeable membranes, which can be employed in the filtration of aqueous solutions and for water purification [55]. The low water absorption of the block copolymers, on the other hand, is attributed to the tremendous hydrophobicity and low surface tension of the siloxanes, due to which the siloxanes come to the air–polymer interface [60] and thus the exposure of polar groups to the polymer surface becomes remarkably low. Such type of copolymers having hydrophobic together with hydrophilic segments can be used in several applications such as the stabilization of emulsions and dispersions of different substances and have the ability to replace low-molecular weight materials in the modification of different surfaces, foaming lubrication and formulation of cosmetics [60].

The isophthaloyl-based organic polyesteramides generally absorb more water compared to their other organic and organometallic counterparts and polyesteramide IA-6 has the highest water uptake value (7.05%) among these polymers probably due to its amorphous nature and presence of more methylene spacers in its backbone compared to other isophthaloyl-based polymers consistent with previously reported observations [61]. It has been reported that polymers containing moieties that aid in rigid close packing exhibit lower water absorption compared to polymers without such groups [62].

Table 4

RMS roughness of the representative copolymers and their respective polyesteramides.

Copolymer	RMS roughness (nm)	Polyesteramide	RMS roughness (nm)
FcBC-5	234.58	FcA-5	1.40
FcBC-6	224.64	FcA-6	1.98
TBC-5	227.16	TA-5	1.65
TBC-6	244.39	TA-6	2.52
IBC-5	239.50	IA-5	2.15
IBC-6	241.25	IA-6	2.43

3.7. XRD analysis

Morphological information on the organometallic copolymers and their organic analogues was obtained from their wide-angle X-ray powder diffraction pattern in the region $2\theta = 0-70^\circ$ at room temperature and the representative X-ray diffractograms of the polymeric materials are shown in Fig. 4. The broad peak patterns of all the synthesized copolymers exhibited that they are amorphous in nature. This may be attributed to the presence of siloxane moiety in the backbone which diminishes the crystallinity [63]. The respective polyesteramides, on the other hand, exhibited variable crystallinity which can be correlated with their structural features. The sharp peak patterns in diffractograms of the terephthaloyl-based polyesteramides in the range $10-40^\circ$ indicated that these are of considerable crystallinity. This indicates that the polymeric chains in the para–para system are symmetric and ordered leading to a more favourable conformation for packing [64]. All the ferrocene-based organometallic polyamides are amorphous in nature as revealed by the diffuse pattern in their diffractograms. This indicates that the introduction of bulky ferrocene moieties in the polyamides decreases the chain–chain interactions, interrupting the close packing of polymer chains and thereby decreasing the crystallinity [65]. The isophthaloyl-based organic polymers were also amorphous in nature as revealed by the typical amorphous hollow pattern in their diffractograms, which shows that the introduction of meta orientation into the polymer chains leads to the distortion of the polymer lattice [57,66]. The X-ray diffraction analysis also reveals that the crystallinity increases with the increase in number of aliphatic spacers in the polymer chain as was evident from the diffractogram of polymer TA-6, which has more reflection peaks compared to that of polymer TA-4. This is explained by the fact that increasing the number of methylene groups in the polymer chain increases the flexibility as well as chain regularity and hence increases the crystallinity [67].

3.8. Surface morphology

The surface of the synthesized block copolymers was examined by scanning electron microscopy (SEM) and atomic force microscopy (AFM), which are complementary techniques used side-by-

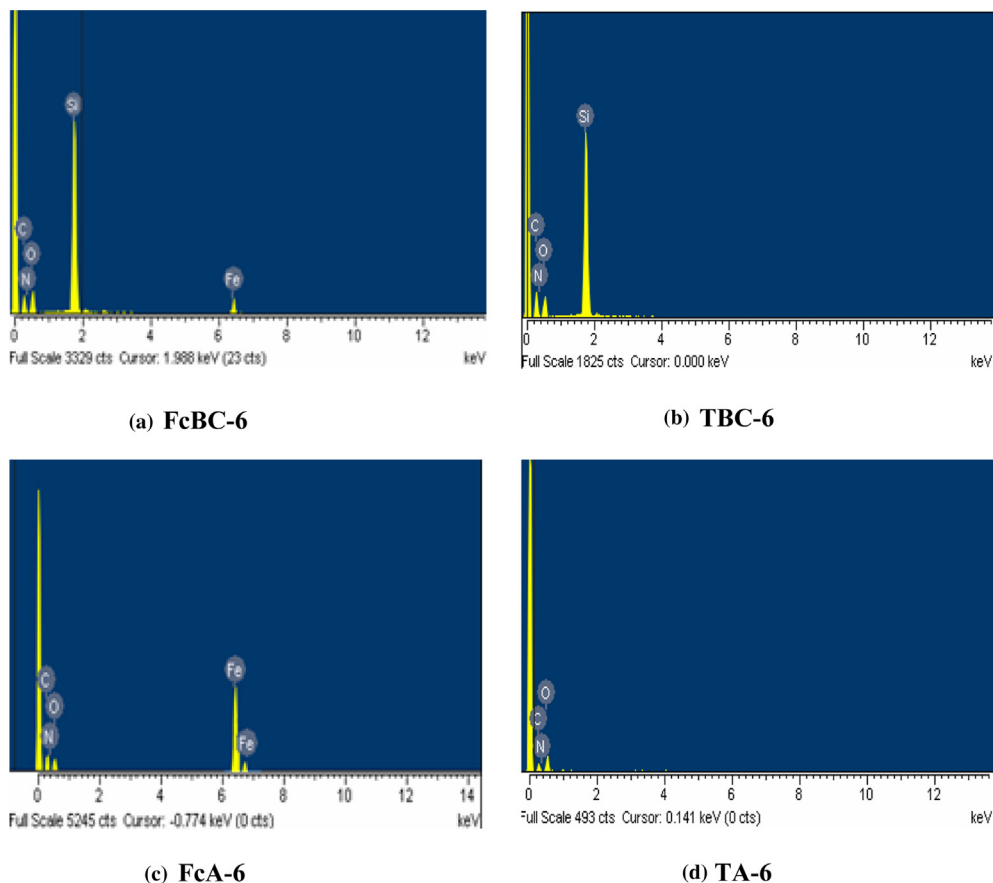


Fig. 7. EDX spectra of representative block copolymers and their corresponding polyesteramide.

side for surface investigations in modern laboratories [68]. The scanning electron micrographs of the block copolymers revealed that most of the surface of the synthesized copolymers was covered by the siloxane segment and microphase separation can hardly be detected. It has been reported that in siloxane-based copolymers with higher siloxane content, the siloxane domains become a dominant part of polymer surface [69]. The micrographs of the selected samples (FcBC-6 and TBC-6) are presented in Figs. 5(a) and (b). The AFM images of the copolymers, Fig. 6(a), also support the argument and the copolymers exhibited high values of surface

roughness (Table 2) due to the migration of siloxane moiety towards the air–polymer interface. This unique feature justifies the use of siloxane-based materials as surface modifiers [70].

The SEM study of the ferrocene-based organometallic polyesteramides revealed that their surface consisted of granular particles while that of the organic polymers consisted of spherical particles. The representative micrographs are depicted in Figs. 5(c) and (d). The AFM images of the synthesized polyesteramides exhibited an almost featureless morphology showing that these polyamides possess smooth surfaces with little roughness (Table 4).

Table 5

DSC results of the synthesized copolymers and their corresponding polyesteramides.

Copolymer	T_g (°C) (soft segment)	T_m (°C) (soft segment)	T_g (°C) (hard segment)	Polyesteramide	T_g (°C)
FcBC-2	–118	–51.50	260	FcA-2	282
FcBC-3	–123	–55.40	262	FcA-3	279
FcBC-4	^a	–52.85	250	FcA-4	271
FcBC-5	–120	–52.30	248	FcA-5	267
FcBC-6	^a	–50.25	255	FcA-6	264
TBC-2	–122	–49.50	262	TA-2	273
TBC-3	^a	–50.85	258	TA-3	270
TBC-4	–118	–51.75	257	TA-4	261
TBC-5	^a	–54.15	255	TA-5	257
TBC-6	–119	–49.55	249	TA-6	251
IBC-2	–124	–51.75	253	IA-2	270
IBC-3	–120	–54.20	247	IA-3	271
IBC-4	–119	–49.55	247	IA-4	259
IBC-5	–124	–51.75	244	IA-5	253
IBC-6	–120	–54.20	241	IA-6	248

T_g = glass transition temperature, T_m = melting temperature.

^a T_g not detected.

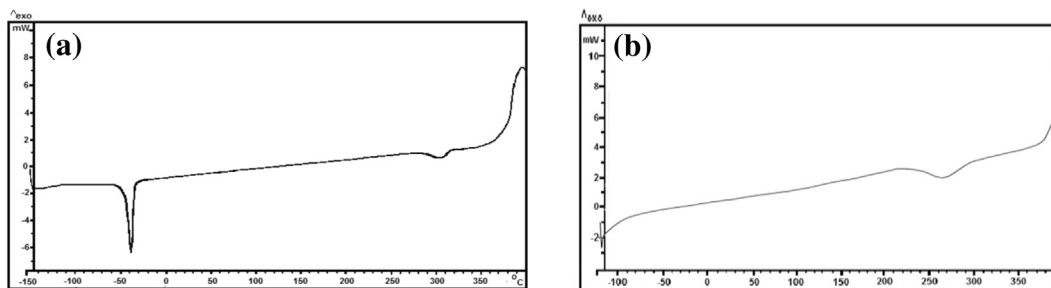


Fig. 8. DSC curves of the synthesized copolymer FcBC-6 (a) and respective polyesteramide FcA-6 (b).

The representative image is given in Fig. 6(b). The EDX patterns of the synthesized organometallic polymers and copolymers also provided evidence for the presence of iron metal in their structure (Fig. 7). The EDX patterns of all the synthesized copolymers confirmed the presence of silicon as well.

3.9. DSC studies

The differential scanning calorimetry (DSC) studies of the synthesized copolymers were carried out at a heating rate of $10\text{ }^{\circ}\text{C min}^{-1}$ in nitrogen. The results obtained for these studies are presented in Table 5. A unique feature of the block copolymers is the microphase separation which is evident from the DSC profiles of the synthesized copolymers (Fig. 8(a)) as both the segments exhibit their representative thermal transitions in the DSC experiments [26,39]. The soft PDMS segment showed a sharp peak at ca. $-50\text{ }^{\circ}\text{C}$ in all the spectra which is attributed to its melting [26,39]. It also exhibited a glass transition temperature (T_g) at ca. $-120\text{ }^{\circ}\text{C}$ [71], which could be detected in most of the spectra. The glass transition temperature (T_g) and melting temperature (T_m) of a polymer are a reflection of the macromolecular chain motion and the amount of free volume in the polymer [72]. The glass transition temperatures of the hard polyesteramide segments are high ($241\text{--}262\text{ }^{\circ}\text{C}$) and could also be observed in the spectra of the synthesized copolymers.

The chain stiffness of the synthesized polyesteramides was characterized by their glass transition temperatures (T_g) obtained from the DSC curves (Fig. 8(b)). The glass transition temperatures of the synthesized polymers were in the range $248\text{--}282\text{ }^{\circ}\text{C}$ in accordance with the reported values of aromatic polyesteramides [73]. The variations in the T_g values could be correlated with the length

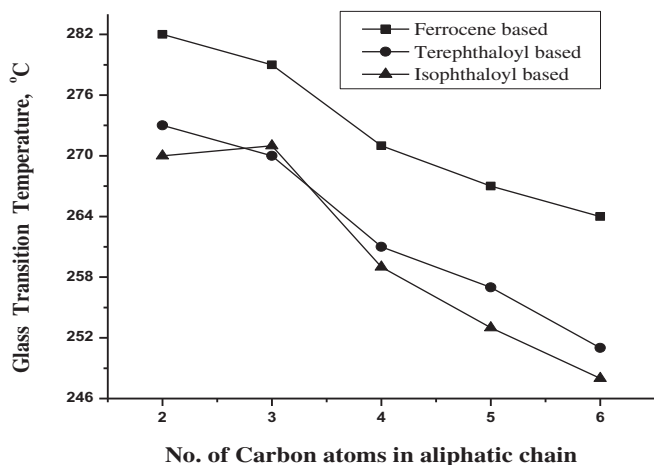


Fig. 9. Plot of T_g vs. no. of carbon atoms in aliphatic chain of the synthesized polyesteramides.

of the aliphatic methylene spacers and the orientation of the phenylene rings. Fig. 9 shows that the glass transition temperatures of the polyesteramides exhibit an essentially linear decrease with increasing methylene chain length. The trend is in line with observations made by earlier workers for polymers containing flexible methylene moieties [16]. The shifting of glass transition temperature values of the respective polyesteramides from those exhibited by the synthesized copolymers indicates the variation in macromolecular chain packing in the block copolymers compared to the homopolymers [71,72].

4. Conclusions

A one-pot two-step solution polycondensation procedure was employed for the synthesis of novel ferrocene-containing siloxane-based block copolymers and their organic analogues. The corresponding polyesteramides of the synthesized block copolymers, without polydimethylsiloxane segment, were also prepared under similar conditions for comparison of properties. All the organometallic and organic block copolymers along with their respective polyesteramides did not melt up to $300\text{ }^{\circ}\text{C}$ and were characterized by their physical properties, FTIR and $^1\text{H NMR}$ spectroscopic techniques, which confirmed the presence all the expected moieties in their macrochain. The synthesized copolymers and polyesteramide materials were soluble in a toluene-THF (1:1) solvent mixture at elevated temperatures and conc. H_2SO_4 at room temperature and possessed low solubility in common organic solvents at room temperature, yet became readily soluble upon N-trifluoroacetylation with trifluoroacetic anhydride. The weight-average molar masses for the synthesized organometallic block copolymers were comparable with those of the organic analogues and were significantly high compared to their respective polyesteramides suggesting that the synthesized block copolymers consisted of multiblocks of hard and soft segments. These block copolymers absorbed very small amounts (ca. 1%) of water compared to their corresponding polyesteramides due to the hydrophobic siloxane moiety and can be used as semi-permeable membranes. Wide-angle XRD studies revealed that all the organometallic and organic copolymers were amorphous in nature, whereas the relevant polyesteramides were of variable crystallinity depending upon their structural features. The surfaces of all the synthesized copolymers exhibited diffused morphology due to the migration of siloxane segment to the surface. The ferrocene-based polyesteramides, on the other hand, exhibited granular morphology while the organic polymers showed spherical surface morphology. The DSC profiles of the synthesized ferrocene-based copolymers and their organic analogues exhibited a phase-separated morphology with two glass transition temperatures (T_g) due to hard polyesteramide and soft polydimethylsiloxane segments. The glass transition temperatures of the ferrocene-based polyesteramides were higher than the organic analogues and

decreased linearly with increase in number of carbon atoms in the aliphatic chain. In conclusion, these studies suggested that the ferrocene-containing siloxane-based organometallic copolymers and their organic analogues generally possessed superior properties and can be utilized in modification of surfaces and in applications where severe conditions requiring high solvent resistance and elevated temperature environments are encountered.

Acknowledgements

The authors would like to thank University Research Fund, Quaid-i-Azam University, Islamabad, for the financial support of this project.

Appendix A. Supplementary material

Supplementary material related to this article can be found at <http://dx.doi.org/10.1016/j.jorgchem.2013.08.002>.

References

- [1] J.M. García, F.C. García, F. Serna, J.L. de la Pena, *Prog. Polym. Sci.* 35 (2010) 623–686.
- [2] M. Trigo-López, P. Estévez, N. San-José, A. Gómez-Valdemoro, F.C. García, F. Serna, J.L. de la Pena, J.M. García, *Recent Patents Mater. Sci.* 2 (2009) 190–208.
- [3] A. Noshay, J.E. McGrath, *Block Copolymers: Overview and Critical Survey*, Academic Press, New York, 1977.
- [4] G. Belorgey, G. Sauvet, *Organosiloxane Block and Graft Copolymers*, in: R.G. Jones, W. Ando, J. Chojnowski (Eds.), *Silicone-containing Polymers*, Kluwer Academic Publishers, The Netherlands, 2000, pp. 43–78.
- [5] Y. Poojari, A.S. Palsule, M. Cai, S.J. Clarson, R.A. Gross, *Eur. Polym. J.* 44 (2008) 4139–4145.
- [6] I.B. Mansour, K. Alouani, E. Chauveau, V. Martin, F. Schiets, R. Mercier, *Eur. Polym. J.* 46 (2010) 814–820.
- [7] S.M. Kulkarni, M.R. Didgikar, R.V. Chaudhari, *J. Mol. Catal. A: Chem.* 207 (2004) 97–106.
- [8] L. Wang, Y. Wang, L. Ren, *J. Appl. Polym. Sci.* 109 (2008) 1310–1318.
- [9] E. Grigat, R. Koch, R. Timmermann, *Polym. Degrad. Stab.* 59 (1998) 223–226.
- [10] C.G. East, V. Kalyvas, J.E. McIntyre, A.H. Milburn, *Polymer* 30 (1989) 558–563.
- [11] A. Banihashemi, H. Toiserkani, *Eur. Polym. J.* 40 (2004) 2783–2791.
- [12] S. Mehdi-pour-Ataei, R. Maleki-Moghaddam, M. Nami, *Eur. Polym. J.* 41 (2005) 1024–1029.
- [13] W. Guo, W.-T. Leu, S.-H. Hsiao, G.-S. Liou, *Polym. Degrad. Stab.* 91 (2006) 21–30.
- [14] Y. Shao, Y. Li, X. Zhao, T. Ma, C. Gong, F. Yang, *Eur. Polym. J.* 43 (2007) 4389–4397.
- [15] S. Mehdi-pour-Ataei, *Eur. Polym. J.* 41 (2004) 91–96.
- [16] J. Yin, Y.F. Ye, Z.G. Wang, *Eur. Polym. J.* 34 (1998) 1839–1843.
- [17] I. Manners, *J. Polym. Sci., Part A: Polym. Chem.* 40 (2002) 179–191.
- [18] N.J. Long, K. Kowalski, *Ferrocene-containing Polymers and Dendrimers*, in: P. Stepnicka (Ed.), *Ferrocenes: Ligands, Materials and Biomolecules*, John Wiley and Sons Ltd., West Sussex, 2008, p. 393.
- [19] G.P. Kittlesen, H.S. White, M.S. Wrighton, *J. Am. Chem. Soc.* 107 (1985) 7373–7380.
- [20] H.Z. Bu, A.M. English, S.R. Mikkelsen, *J. Phys. Chem. B* 101 (1997) 9593–9599.
- [21] N.C. Foulds, C.R. Lowe, *Anal. Chem.* 60 (1988) 2473–2478.
- [22] P.D. Hale, L.I. Boguslavsky, T. Inagaki, H.I. Karan, H.S. Lee, T.A. Skotheim, *Anal. Chem.* 63 (1991) 677–682.
- [23] W. Li, N. Sheller, M.D. Foster, D. Balaishis, I. Manners, B. Annis, J.S. Lin, *Polymers* 41 (2000) 719–724.
- [24] E.W. Neuse, *J. Inorg. Organomet. Polym.* 15 (2005) 3–31.
- [25] M.E. Wright, E.G. Toplikar, R.F. Kubin, M.D. Seltzer, *Macromolecules* 25 (1992) 1838–1839.
- [26] T. Kausar, M. Mazhar, G.B. Shah, M. Ali, S. Ali, *Main Group Metal Chem.* 23 (2000) 351–360.
- [27] A. Kaiser, H. Schmidt, H. Bottner, *J. Membr. Sci.* 22 (1985) 257–268.
- [28] P. Vondráček, B. Doležel, *Biomaterials* 5 (1984) 209–214.
- [29] R. Gill, M. Mazhar, O. Félix, G. Decher, *Angew. Chem., Int. Ed.* 49 (2010) 6116–6119.
- [30] C. Wu, K.Q. Xia, *Rev. Sci. Instrum.* 65 (1994) 587–590.
- [31] A.L. Stanton, R.A. Storer, E.D. Cannon, *ASTM Standard Test Method for Water Absorption of Plastics: Designation D570-81*, in: *Annual Book of ASTM Standards*, American Society of Testing and Materials, Philadelphia, PA, 1990.
- [32] M. Rosenblum, R.B. Woodward, *J. Am. Chem. Soc.* 80 (1958) 5443–5449.
- [33] F.W. Knobloch, W.H. Rauscher, *J. Polym. Sci.* 54 (1961) 651–656.
- [34] M.S.U. Khan, A. Nigar, M.A. Bashir, Z. Akhter, *Synth. Commun.* 37 (2007) 473–482.
- [35] M.A. Mohsin, Z. Akhter, M. Bolte, M.S. Butt, M.S.U. Khan, H.M. Siddiqi, *J. Mater. Sci.* 44 (2009) 4796–4805.
- [36] B.S. Furniss, A.J. Hannaford, P.W.G. Smith, A.R. Tatchell, *Vogel's Text Book of Practical Organic Chemistry*, fifth ed., Longman Company Ltd, Harlow, 1989.
- [37] D.L. Pavia, G.M. Lampman, G.S. Kriz, *Introduction to Spectroscopy*, third ed., Thomson Learning Inc., New York, 2001.
- [38] J.M. García, F.C. García, F. Serna, *J. Polym. Sci., Part A: Polym. Chem.* 41 (2003) 1202–1215.
- [39] R. Gill, M. Mazhar, M. Siddiq, *Polym. Int.* 59 (2010) 1598–1605.
- [40] N. Ogata, T. Ikari, *J. Polym. Sci., Polym. Chem. Ed.* 11 (1973) 1939–1952.
- [41] J. Preston, F. Dobinson, *J. Polym. Sci., Part B: Polym. Lett.* 2 (1964) 1171–1174.
- [42] A.S. Patil, M. Medhi, N.V. Sadavarte, P.P. Wadgaonkar, N.N. Maldar, *Mater. Sci. Eng., B* 168 (2010) 111–116.
- [43] B. Kaczmarczyk, *Polymer* 39 (1998) 5853–5860.
- [44] A. Borriello, L. Nicolais, S.J. Huang, *J. Appl. Polym. Sci.* 95 (2005) 362–368.
- [45] M. Cazacu, A. Vlad, M. Marcu, C. Racles, A. Airinei, G. Munteanu, *Macromolecules* 39 (2006) 3786–3793.
- [46] J.R. Sargent, W.P. Weber, *Polymer* 40 (1999) 3795–3802.
- [47] E. Jacobi, H. Schuttenberg, R.C. Schultz, *Makromol. Chem., Rapid Commun.* 1 (1980) 397–402.
- [48] B.H. Zimm, *J. Chem. Phys.* 16 (1948) 1099–1116.
- [49] S. Zulfiqar, I. Lieberwirth, M.I. Sarwar, *J. Chem. Phys.* 344 (2008) 202–208.
- [50] T. Otsuki, M. Kakimoto, Y. Imai, *Polym. J.* 24 (1992) 347–355.
- [51] S.C. Yu, S. Hou, W.K. Chan, *Macromolecules* 33 (2000) 3259–3273.
- [52] R.B. Seymour, C.E. Carraher Jr., *Polymer Chemistry: An Introduction*, Marcel Dekker Inc., New York, 1981.
- [53] M.R. Pixton, D.R. Paul, *Polymer* 36 (1995) 2745–2751.
- [54] G.-S. Liou, S.-H. Hsiao, M. Ishida, M. Kakimoto, Y. Imai, *J. Polym. Sci., Part A: Polym. Chem.* 40 (2002) 2810–2818.
- [55] V. Ayala, E.M. Maya, J.M. García, J.G. de La Campa, A.E. Lozano, J. de Abajo, *J. Polym. Sci., Part A: Polym. Chem.* 43 (2005) 112–121.
- [56] C.L. Zhang, L.F. Feng, X. Gu, S. Hoppe, G.H. Hu, *Polym. Test.* 26 (2007) 793–802.
- [57] R. Takatsuka, K. Uno, F. Toda, I. Yoshio, *J. Polym. Sci., Polym. Chem. Ed.* 15 (1977) 1905–1915.
- [58] S. Zulfiqar, Z. Ahmad, M.I. Sarwar, *Colloid Polym. Sci.* 285 (2007) 1749–1754.
- [59] E. Rusu, M. Onciu, *Des. Monomers Polym.* 8 (2005) 37–47.
- [60] M. Scibiorek, N.K. Gladkova, J. Chojnowski, *Polym. Bull.* 44 (2000) 377–384.
- [61] J.G. de La Campa, E. Guizarro, F.J. Serna, J. de Abajo, *Eur. Polym. J.* 21 (1985) 1013–1019.
- [62] S. Bhuvana, M. Madhumathi, M. Sarojadevi, *Polym. Bull.* 57 (2006) 61–72.
- [63] X. Jiang, J. Gu, Y. Shen, S. Wang, X. Tian, *Desalination* 265 (2011) 74–80.
- [64] V.L. Rao, P.V. Prabhakaran, *Eur. Polym. J.* 28 (1992) 363–366.
- [65] S. Mehdi-pour-Ataei, S. Babanzadeh, *React. Funct. Polym.* 67 (2007) 883–892.
- [66] S.-H. Hsiao, Y.-J. Chen, *J. Polym. Res.* 7 (2000) 205–213.
- [67] K.I. Aly, M.A. Abbady, S.A. Mahgoub, M.A. Hussein, *Express Polym. Lett.* 1 (2007) 197–207.
- [68] F.M. Mirabella Jr., A. Weiskittel, *Polym. News* 30 (2005) 143–148.
- [69] N. Furukawa, Y. Yamada, M. Furukawa, M. Yuasa, Y. Kimura, *J. Polym. Sci., Part A: Polym. Chem.* 35 (1997) 2239–2251.
- [70] M. Bouteau, S. Cantin, O. Fichet, F. Perrot, D. Teyssie, *Langmuir* 26 (2010) 17427–17434.
- [71] I.M. Raigorodskii, E.S. Gol'dberg, *Russ. Chem. Rev.* 56 (1987) 1079–1095.
- [72] H.R. Allcock, R. Prange, *Macromolecules* 34 (2001) 6858–6865.
- [73] G.-S. Liou, S.-H. Hsiao, *J. Polym. Sci., Part A: Polym. Chem.* 40 (2002) 2564–2574.